Imaging Optodes

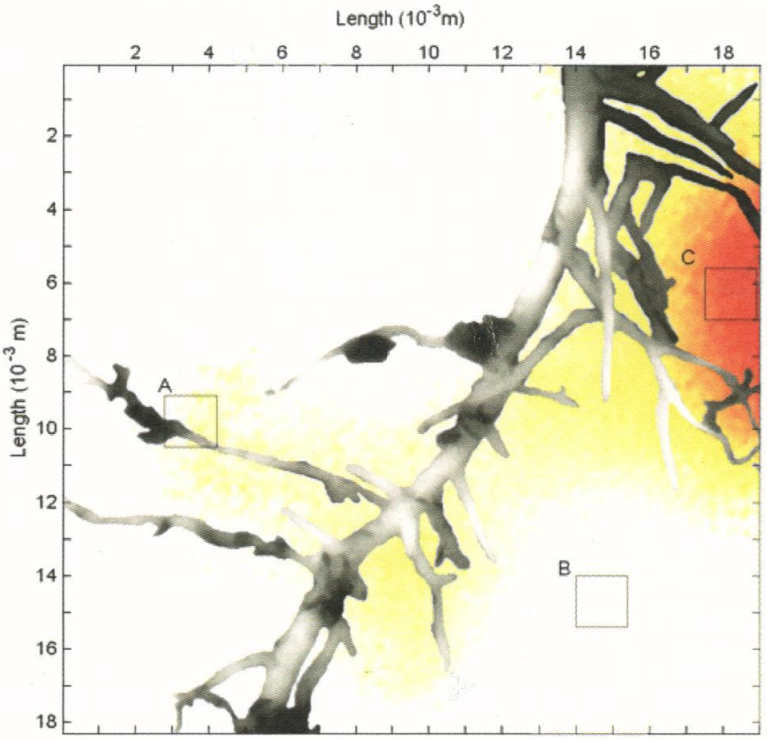

NIKLAS STRÖMBERG

Department of Chemistry
Analytical Chemistry
Göteborg University

GÖTEBORG UNIVERSITY

Imaging Optodes

NIKLAS STRÖMBERG

AKADEMISK AVHANDLING

för filosofie doktorsexamen i kemi (examinator: Professor Daniel Jagner), som enligt beslut av tjänsteförslagsnämden, Institutionen för Kemi vid Göteborgs Universitet, kommer att försvaras fredagen den 9:e juni 2006, kl. 10.15 i föreläsningssal KA, Kemigården 4, Göteborgs Universitet och Chalmers Tekniska Högskola, Göteborg.

Fakultetsopponent: Associate Professor Richard B. Thompson, Department of Biochemistry and Molecular Biology, University of Maryland School of Medicine, USA.

Department of Chemistry
Analytical Chemistry
Göteborg University
2006

Abstract

Imaging Optodes
Niklas Strömberg, Department of Chemistry, Analytical Chemistry, Göteborg University, SE-412 96 Göteborg, Sweden

One of the major benefits from optical sensors with chemical recognition (optodes) is that signals can be transferred to imaging sensors. The often small-scale, non-steady-state and heterogeneous characteristics of natural environments make imaging optodes an interesting complement, or alternative, to ion-selective electrodes for reversible detection of solute concentrations. The general principle of imaging optodes is to immobilize solute specific fluorescent indicators onto/within thin-layered plastic films. The sensor film in contact with the sample is illuminated and images of the fluorescence intensities are captured with a camera.

The overall objective of this study was to develop and characterize the basic analytical performance of an imaging optode (planar fluorosensor) for continuous measurements of ammonium concentrations in complex environments like sediments and soils. The response time of the developed imaging optode was less than 4 minutes and the optode was able to reversibly sense ammonium from μM to mM concentrations using a novel phase ratiometric approach. The detection limit was ~ 1×10^{-6} M, i.e. about the same or even better than that of the best performing ion-selective electrodes for ammonium. In addition, the sensor was found pH independent with an enhanced selectivity to ammonium (NH_4^+:K^+ ~ 17:1) compared to potassium. The long-term drift in ratio was efficiently eliminated using a time correlated pixel-by pixel-procedure. The same procedure facilitated control of sensor parameters such as analytical sensitivity, limit of detection and operational lifetime at a pixel resolution.

Studies of ammonium turnover close to a root system of a tomato plant, and dissolution of long-term fertilizers in soil, exemplify the non-destructive procedure and large potential of high-resolution imaging in natural environments.

KEYWORDS: Imaging optodes, planar optodes, optode, ammonium, sensing, sensor

ISBN 91-628-6848-9

Populärvetenskaplig sammanfattning på svenska

En avbildande optod (imaging optode) är en sensorfilm som med hjälp av ljus reversibelt detekterar ett kemiskt ämne över tiden. Tekniken, som ännu så länge är begränsad till mätningar av syrgas och vätejoner, har endast funnits i 10 år och används idag flitigt av forskare för att studera fördelningen av dessa ämnen i sediment och andra komplexa matriser.

Den generella principen för en avbildande optod är att inkorporera ett fluorescerande färgämne, känsligt för analyten, i en plastfilm. Filmen i fysisk kontakt med det objekt man vill studera belyses med ljus av specifika våglängder och bilder av den efterföljande fluorescensintensiteten tas med en kamera. Fluorescensen utnyttjas på olika sätt som ett mått på koncentrationen av ämnet i provet. Svårigheten med att konstruera sådana filmer är att hitta lämpliga detektionsprinciper för analyten. Vidare bör man inte direkt utnyttja fluorescensintensiteten eftersom denna påverkas av t.e.x. variationer i excitationsljus, ojämn fördelning av det analytkänsliga färgämnet och fluktuationer i känslighet hos kamerasystemet.

Denna avhandlig beskriver den gradvisa utvecklingen av en avbildande optod för ammonium. Optoden baserar sig på en nyutvecklad fasratiometrisk detektionsprincip (normaliseringsmetod) och är därmed oberoende av fluorescensintensiteten. Den utvecklade optoden med tillhörande kalibreringsteknik möjliggör pH-oberoende, selektiv samt drift-fri detektion av låga halter (µM) ammonium över tiden i bildformat. Vidare utnyttjas kalibrertekniken för att ge mått på sensorns prestanda i varje pixel genom bilder som återger analytisk känslighet och detektionsgräns vid den tidpunkt då experimentbilden är tagen. Tekniken blir extra intressant då det är lätt att modifiera optoden till mängd andra ämnen.

Det kraftfulla mätförfarandet återspeglas framförallt i ett av de experiment som finns beskrivna i avhandlingen där ammoniumkoncentrationer kring ett rotsystem studerades över tiden. På detta sätt kunde omsättningshastigheten för ammonium vid olika tillfällen på dygnet bestämmas. Bilderna speglar också balansen mellan upptag och tillskott av ammonium kring rötter där det bland annat visade sig att rotkonfigurationen hade avgörande betydelse för utvecklandet av utarmningszoner kring rotstrukturerna.

Kväve och fosfor utgör två av de viktigaste näringsämnena för växter, där ammonium utgör den mest eftertraktade kväve formen. Detta har sedan 1940 talet utnyttjats för att öka tillväxten av grödor på våra åkrar. Den ökade användningen av konstgödsel har dock orsakat övergödning av våra sjöar och kustnära hav. Även om fosfathalterna minskade drastiskt under 1980-talet p.g.a. införandet av fosfatfria tvättmedel och effektivare reningsmetoder i reningsverken, så har en motsvarande minskning inte skett för kväve. Detta beror troligtvis på att kvävetillskottet till största delen kommer ifrån diffust läckage från åkrarna och inte från punktutsläpp från hushåll och industrier. Förhoppningsvis kan avbildande optoder erbjuda nya möjligheter för mätning av mängd olika analyter i komplexa miljöer för att öka förståelsen för hur ämnen sprids och omsätts i naturen.

Part A

Part B

Research papers

Papers included in the thesis (referred to in text by their Roman numerals):

Paper I Strömberg N, Hulth S
Ammonium selective fluorosensor based on the principles of coextraction
ANALYTICA CHIMICA ACTA 443 (2): 215-225 SEP 17 2001

Paper II Strömberg N, Hulth S
A fluorescence ratiometric detection scheme for ammonium ions based on the solvent sensitive dye MC 540
SENSORS AND ACTUATORS B-CHEMICAL 90 (1-3): 308-318 Sp. Iss. SI APR 20 2003

Paper III Strömberg N, Hulth S
Assessing an imaging ammonium sensor using time correlated pixel-by-pixel calibration
ANALYTICA CHIMICA ACTA 550 (1-2): 61-68 SEP 26 2005

Paper IV Strömberg N, Hulth S
Time correlated pixel-by-pixel calibration for quantification and signal quality control during solute imaging
SENSORS AND ACTUATORS B-CHEMICAL 115 (1): 263-269 MAY 23 2006

Paper V Strömberg N
Determination of ammonium turnover close to roots using imaging optodes (manuscript)

Introduction

In quantitative analytical chemistry, measurements ideally represent analyte concentrations in a three-dimensional space over time. However, most analytical methods are based on discrete sampling (often destructive protocols), which normally disrupts the ideal representation of the analyte. The emphasis of this thesis is to describe and provide a brief overview of alternative detection schemes for solutes in natural environments. Main focus includes imaging techniques for high-resolution, continuous and reversible measurements of solutes in complex matrixes, such as soil and aquatic sediments. Thereby, comprising four out of five possible dimensions of an ideal measurement, i.e. two in space, the measured concentration and time. The progressive development of an imaging ammonium optode and test-applications of the sensor are described in Papers I-IV included in the thesis. The resulting imaging technique and imaging optode (planar fluorosensor) was used to measure ammonium distribution close to tomato roots over time (Paper V).

Nitrogen and phosphorous are two of the most important macronutrients for photosynthetic organisms, where ammonium constitute the most easily metabolised nitrogen specie[1,2]. N and P are most often growth-limiting for plants and ever since 1940, effective fertilizers have been widely used in agriculture to increase crop growth[3,4]. However, the extended use has created environmental side-effects. Leakage of nutrients from the enriched soils to adjacent areas such as lakes, rivers and coastal marine environments has caused enhanced growth of aquatic vegetation or phytoplanktic material that disrupts the normal functioning of the ecosystem. However, during the 1980s a vast reduction of phosphorus discharge was made through efficient sewage treatment and introduction of phosphate free detergents. Unfortunately, despite large efforts to reduce overall input of N from sewage treatments, a corresponding decrease of nitrogen is more difficult to establish due to a significant river supply and diffusive drainage of soils rather than discharge from households and industries[3]. Therefore, imaging of nitrogen species concentrations and rates of turnover directly in soil and sediments makes it possible to explore the relation between uptake and supply of ammonium to plants at a high temporal and spatial resolution. Ultimately, such studies improve the overall understanding of ammonium turnover in these complex environments and thereby minimize the environmental hazards associated with fertilizer applications.

Historical background

The idea to determine sample characteristics such as particle and solute concentrations by the properties of light is not recent. The first experiments on the behavior of light in liquids were most likely performed by August Beer in 1852, probably supported by the findings of light absorption in the atmosphere by Pierre Bouguer in 1729 and Johann Heinrich Lambert in 1760. These early investigations on the properties of light led to the well-known Beer-Lambert law (Eq. 1) that describes the fundamental relations between solute concentration and light absorption.

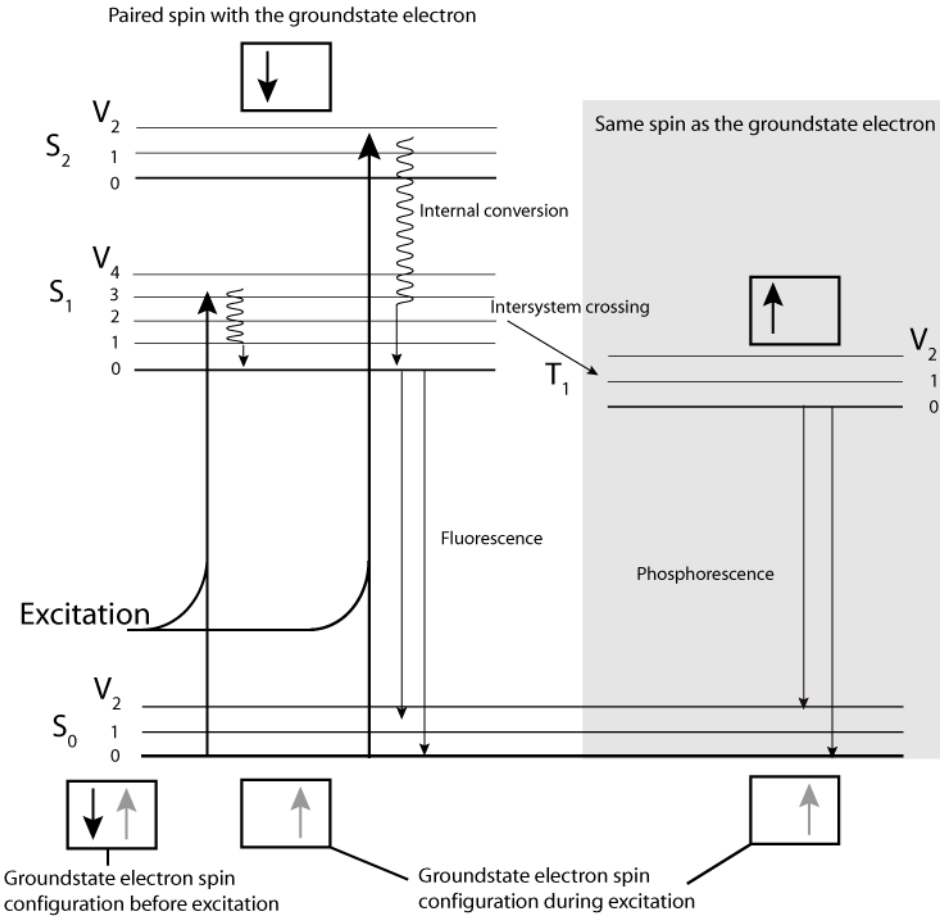

Figure 1. The Jablon´ski diagram, illustrating the principles of fluorescence and phosphorescence. Subsequent excitation to a vibration level (V_x) in singlet excited states (S_1, S_2) the electron relaxes to the lowest level in S_1 (internal conversion). Fluorescence is the luminescent process from the lowest vibration level in S_1 to one of the vibrational levels in the ground state (S_0). The process in which the electron changes spin orientation relative to the ground state during the exited state is called intersystem crossing. Phosphorescence is the emissive process from the lowest vibrational level in the triple state (T_1).

More than a century after the discovery of light absorption, Sir John Frederick William Herschel reported (1845) the first observation of fluorescence[5]. He recognized a blue coloration of an initially colorless quinine solution upon exposure to sunlight. Seven years later, a more or less identical experiment was performed and

more thoroughly evaluated by Sir George Gabriel Stokes[6]. In the study "*On the change of refrangibility of light*", he discussed the wavelength shift (Stokes´ shift) to longer wavelengths subsequent to excitation, and more general relations between excitation and emission of light.

A molecule in its ground state has the electrons organized in pairs of opposite spin-orientations. Fluorescence is emission of light from the singlet (S_1) state to the ground state in which the excited electron has the opposite spin orientation compared to the electron in the ground state (Figure 1). The emissive processes to the ground state of electrons with the same spin as the ground state electron is called phosphorescence. The process is not "spin-allowed" and the emissive rate is therefore much slower compared to fluorescence i.e. 10^3 to 1 s^{-1} (phosphorescence) compared to 10^8 s^{-1} (fluorescence)[7]. A Jablon´ski diagram illustrates the processes after light absorption (Figure 1).

$$A = \lg\frac{I_0}{I} = \varepsilon * l * c \qquad \text{(Eq. 1)}$$

$$\lg\frac{I_0}{I} = OD \qquad \text{(Eq. 2)}$$

A	absorbance
I_0	incident light intensity
I	remaining light intensity
ε	molar absorptivity
l	path length
c	species concentration
OD	optical density

Stokes suggested that optical phenomena, such as light absorption, reflection and fluorescence could be used to identify and quantify organic substances[6,7]. His ideas were not realized until World War II, when the US Department of Defense was interested in monitoring antimalaria drugs, including quinine. This economical input and scientific focusing led to the development of the first spectrofluorometers in the 1950s.

Absorbing species and scattering of light within the sample cause deviation from the overall principles of Beer-Lambert law. The sum of these effects is generally referred to as optical density or inner-filter effects (Eq. 2). Thus, the sample needs to be free from scattering particles in order to measure absorbance of the analyte and accurately relate absorbance to solute concentration. According to Eq. 2, an infinitely diluted solution approaches an optical density of 0.

Besides the possibility to determine species concentrations, light can be used to determine particle size and turbidity of solutions. Particles scatter light (the Tyndall effect) with patterns depending on the shape and size of the particles[8]. Already in 1871, Lord Rayleigh, laid the foundation for the theoretical principles of light scattering by applying the electromagnetic theory of light to small, non-absorbing spherical particles in a gaseous medium. The electromagnetic behavior of light induces oscillating dipoles within a polarizable insulating (non-absorbing) spherical particle. If the particle diameter is less than $\lambda/20$, the particle acts as a point source

and emits light of identical wavelength as the incident light beam (i.e. Rayleigh scattering)[9]. The scattering intensity is inversely proportional to λ^4, causing blue light ($\lambda\sim$ 450 nm) to be more scattered than red light ($\lambda\sim$ 650 nm). If the particle size is larger, or equivalent to, the incident wavelength, the particle is no longer thought of as a point source. Emission of light from different areas of the particle surface may diffract or totally quench the emitted light. These latter phenomena are known as Debey ($d \sim\lambda/20$) and Mie scattering ($d >\lambda/20$)[8].

Although the fundamental laws of light have remained relatively intact over the years, analytical techniques and bench-top instrumentation have dramatically improved the last 50 years or so. Furthermore, the development of optical components such as photo diodes, diode lasers, light emitting diodes (LED) and optical fibers has created new opportunities to detect solutes of low concentrations with high precision and accuracy. These components also facilitate miniaturization of analytical instruments and open up new ways for analyte detection. Moreover, the successive development of highly sensitive and low-cost imaging sensors like charge-coupled devices (CCD) and complimentary metal-oxide semiconductors (CMOS) has made it possible to image solutes directly in complex matrixes. Since the introduction on the market in the 1970s, the rapid and widespread development of highly light-sensitive imaging sensors has radically reduced both price and size of the components. However, development and implementation of analytical techniques based on these components to quantify analytes *in-situ* and *in-vitro*, have just begun.

Terminology

Spectroscopy can be used for qualitative and quantitative studies of chemical compounds and physical properties. In qualitative spectroscopy, molecular structures or chemical bonds are typically of interest. Commonly used techniques for structure determinations include nuclear magnetic resonance (NMR) and infrared spectroscopy (IR). Raman spectroscopy is usually used qualitatively, although quantitative measurements can be performed through multivariate evaluation techniques[10-12]. In quantitative spectroscopy, the concentration of a specific compound is determined using the properties of light. Furthermore, direct spectroscopic techniques are frequently used to measure e.g. intrinsic absorption, scattering, or fluorescence associated with the analyte. However, most analytes do not possess light characteristics appropriate for direct detection and even if so, solute quantification in a mixture of compounds requires light properties specific for the analyte. Therefore, most analytes need to be measured indirectly according to wet chemical procedures that mediate a change in light properties directly related to the solute concentration. Reagent-mediated spectroscopic techniques are often classified as sensors or probes. A sensor is a device that continuously and reversibly measures a physical parameter or chemical concentration over time. Although not unambiguously defined among disciplines in science, a probe is normally irreversible and instantaneous[8]. The general difference between sensors and probes can be exemplified by the pH glass electrode (sensor) and the pH indicator test strip (probe). If measurements over time are not crucial in the experiment, probes (test strips) often offer a calibration-free and

convenient way for semi-quantitative analyte detection. To quantify substances in solutions, absorbance and fluorescence measurements generally require the sample to be diluted and free from scattering particles to avoid inner filter effects. However, if the reagents used for sensing of an analyte are immobilized in, or covered by, a thin protective polymer matrix, negative interaction between the sensor and the sample as well as importance of the inner filter effects are minimized. This configuration is called "optode" ("optical way" in Greek) or sometimes optrode, a combination of "**op**tical and elec**trode**"[13-15]. The technique using immobilized reagents facilitates solute imaging in complex environments such as sediments, soils and cells. The first optode was made for determination of oxygen in 1968 by quenching of the fluorescence from fluoranthene directly soaked on glass[16] (Figure 2). Fluoranthene incorporated in polymer matrixes such as silicone, natural rubber or polyethylene was also tested at this time but resulted, however, in a slower and decreased response to oxygen. The optode was assembled in a gas-tight flow cell and illuminated by an UV-emitting glow lamp. A light detector captured fluorescence through an UV-absorbing filter. The setup also included a reference detector to avoid variations in light intensities of the light source.

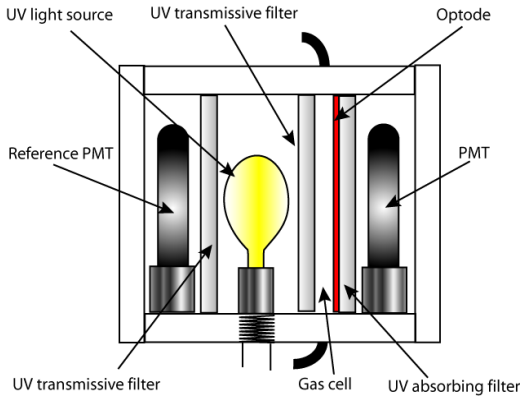

Figure 2. The first optode configuration redrawn from patent GB1190583 but modified to include photo multiplicator tube (PMT) instead of cadmium sulphide photoconductive cell (also covered by the patent description). The optode was used for detection of atmospheric oxygen injected in the gas cell.

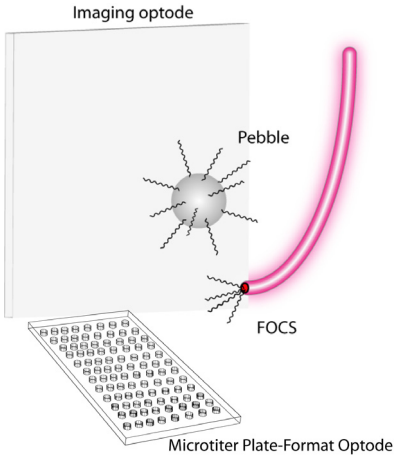

Figure 3. Different optode designs.

Optode designs

Optical fibers are based on total internal reflection of light in a core of a higher refractive index than the surrounding cladding. In 1970, researchers at the Corning Glass Works produced a silica fiber with a light transmission efficiency about 1 % over a distance of 1 km. In 1982, the transmission rose to about 96% over the same distance[17]. Optical fibers offer superior light guiding properties that have been exploited for sensing applications in the environment, in vivo as well as in microscopy. Optodes have been applied both within the cladding and on the distal end of fibers, i.e. fiber optic chemical sensors (FOCS). Main advantages for environmental sensing using FOCS include remote sensing at multiple locations offering extensive replication over time with minimal disturbances. The smallest diameters of commercial optical fibers are about 50 μm and therefore too large for many sensing applications. Measurements inside single cells have been facilitated by the use of fiber-tip nano optodes[18] where the end of the fiber has been stretched to ~40 nm[19]. However, the ability to measure multiple analytes in small compartments (e.g. cells) is severely limited by the number and size of the fibers that could be inserted without altering the cell function. The "pebble" (probes encapsulated by biologically localized embedding) sensor utilizes ratiometric fluorescent dyes confined in 20-200 nm polyacrylamide spheres (Figure 3) for intracellular studies of e.g. pH and calcium[20,21]. Pebbles specific for H^+ and Ca^{2+}, respectively, have been microinjected into the single cell for simultaneous detection of these solutes. The pebble matrix was found biocompatible and protected the fluorescent dyes from interferences and interactions by e.g. proteins in the cell. Another useful application for optodes is found in the medical intensive care for analysis of blood electrolytes where there is a need for fast, easy and reliable analysis of especially potassium sodium and calcium[22]. For rapid clinical studies, optodes have also been assembled in a microtiter plate format by employing an ordinary microtiter plate reader[23]. The practical utility of microtiter plate-format optodes was examined for high throughput screening (100 samples within 5 min) of sodium and potassium in blood serum samples[23].

Most likely due to the focus of applying optodes in combination with optical fibers, optodes designed for spatial determinations of solutes (imaging optodes) were not introduced until 1996[24]. Until this time, optodes were routinely used in combination with optical fibers or directly in spectrofluorometers. The general principle of fluorescence imaging optodes is to immobilize solute specific fluorescent dyes onto/within thin-layered plastic films. The sensor film in contact with the sample is illuminated at specific wavelengths and images of the fluorescence intensities are captured with a camera (Figure 13). To reflect that the optode film was used for imaging the sensor set-up was referred to as a planar optrode. However, objections to this terminology include that reagents were immobilized on plane glass or in a film already in the original design from 1968 (Figure 2) and that many FOCS have reagents organized in a planar geometry. In addition, it neither follows the generic term for light detectors nor optics used for imaging. In this thesis, films that reversibly image solute concentrations over time using light for signal transduction to an imaging sensor (CCD) are denoted as ***imaging optodes***.

Detection principles suitable for imaging optodes

Since the introduction of imaging optodes for solute quantification in complex environments like sediments and soils, most (if not all) sensing schemes make use of fluorescence properties. As fluorescence and direct quantification of analytes using fluorescence intensities are associated with leakage and photo bleaching of the dye, additional and complementary techniques to image solutes reversibly over time are desirable. During solute imaging of analytes in complex environments, the opposite side of the sensor film is illuminated compared to where analytes interact with the sensing film. The sections below give a brief overview of possible additional and complementary detection schemes that could be used (some have been used) in the design of imaging optodes based on finite imagery, i.e. many single point sources of rays combine to form a continuous finite object at the detector at the same time. Thus, no scanning devices and only techniques that have the potential to be used with imaging optics are discussed.

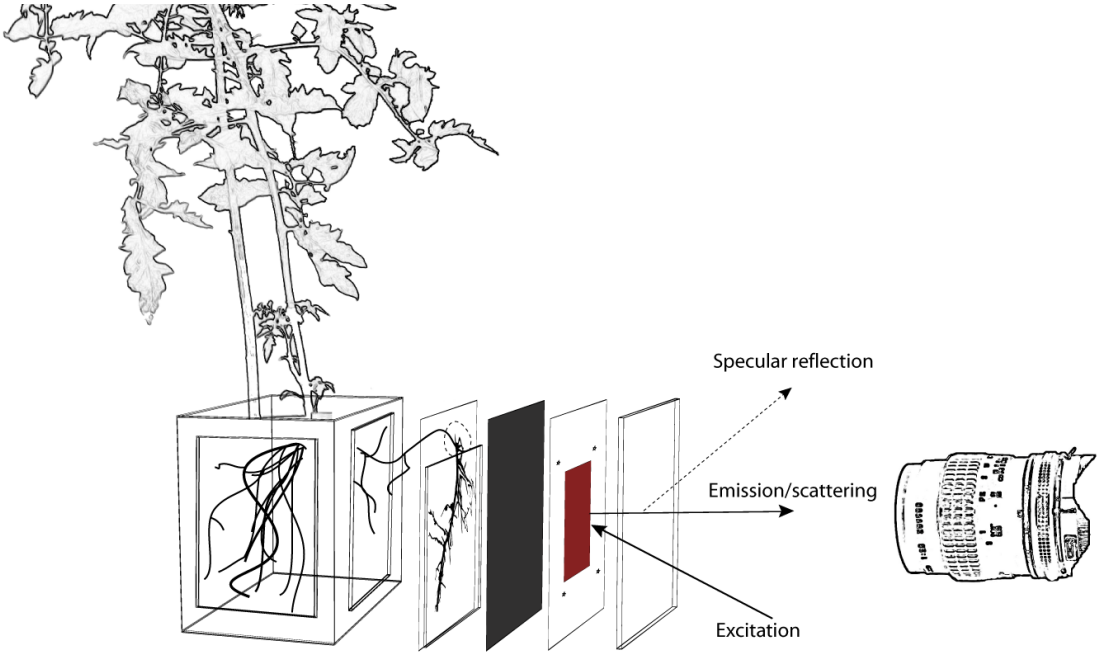

Figure 4. Imaging optode assembly for detection of solutes in complex matrices. The sensor film is illuminated and detected from the opposite side of where analytes interact with the sensing film.

Reflectometry and refractometry

Diffuse reflectance

Reflectance is the ratio of the reflected intensity to the incident intensity, generally expressed in decibels or percentage at the surface of a material[17]. Reflectance measurements are normally performed in a spectrofluorometer using barium sulfate as reference standard of the incident light intensity[25].

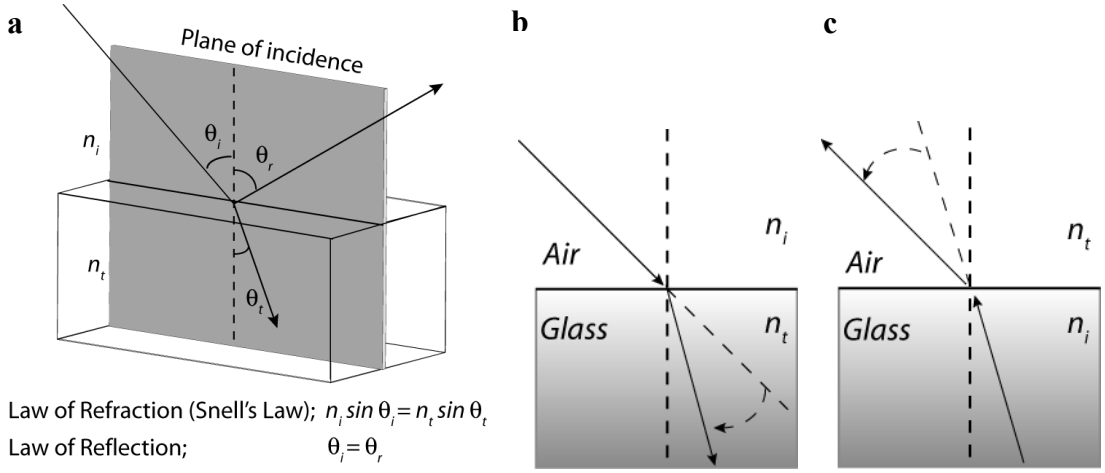

Figure 5. Refraction and reflection of light on a flat surface. The incidence, reflected, and transmitted beams each lie in the plane of incidence (**a**). When a beam of light enters a more optically dense medium (**b**), one with a greater index of refraction ($n_i<n_t$), it bends towards the perpendicular. When a beam goes from a more dense to a rare medium ($n_i>n_t$), it bends away from the perpendicular (**c**).θ_i, θ_r and θ_t denote angles of incident, reflected and transmitted light, respectively.

Light impinging on a smooth and flat surface of an optically dense medium will generally reflect and refract rays according to the laws of reflection and refraction, respectively (Figure 5). The reflected specular rays are normally of limited use in a sensing perspective and are therefore often directed away from the detector to avoid over-exposure. The refracted rays are either absorbed or scattered by the material. If the dense material is completely transparent, a reflecting surface or scattering particles must be incorporated in the sensor for diffusive reflectance measurements. Presence of absorbing analytes in the region of the refracted rays reduces the scattering intensity and thereby decreases the diffuse reflectance from the sample. Sensing schemes for insulating (non-absorbing) analytes could be designed by using a reagent that reversibly induces an increased or decreased absorption when exposed to the analyte. In addition, other parameters of the scattered light such as spectral change, angular distribution and polarization could be utilized for analyte detection. The Beer-Lambert's law (Eq. 1) is generally sufficient to describe the response from such sensor designs[26]. However, absorbance measurements require that the intensity of transmitted light is determined without the presence of the light-absorbing compound (i.e. blank measurement), which is hard to accomplish due to the general configuration of optodes. This drawback has been corrected for by retrieving the intensity from a non-absorbing wavelength, and use this intensity as I_0[26] (Eq. 1). Kubelka and Munk have developed a theory for direct quantification of analytes using the absolute (i.e not normalized to the incident light intensity) reflectance spectra from thick dense opaque materials[27] (Eq. 3). Compared to absorbance measurements and quantification of solute concentration according to Beer-Lambert´s law (Eq. 1), reflectance measurements have a wider dynamic range[28] which is desirable in a sensor design. Regardless theoretical concerns of the response, the concentrations could be determined using the normalized intensity of the reflected light (Eq. 4)[29] plotted versus analyte concentrations. However, the response might become non-linear.

$$C = \frac{S(1-R_a)^2}{2R_aK} \quad \text{(Eq. 3)}$$

$$R_N = \frac{R - R_{\min}}{R_{\max} - R_{\min}} \quad \text{(Eq. 4)}$$

R_a	reflected intensity in presence of analyte, i.e. background subtracted
C	analyte concentration
S	scattering constant
K	absorption constant
R_N	normalized reflected intensity
R_{max}	highest reflected intensity
R_{min}	lowest reflected intensity

Examples of optodes based on diffuse reflectance include mainly FOCS for pH detection[26,27,29,30]. The best performing sensor had a linear response in pH from 4.9 to 10.5, a precision of ± 0.01 pH units, and about 5 min response time. A test of a similar fiber optic pH sensor in turbid solutions induced only slight changes in reflectance, indicating the usefulness of diffuse reflectance in complex environments[29]. Diffuse reflectance has also been used for detection of trace levels of nitrite (0,1 ng/ml) in conjunction with solid phase extraction in a flow through cell and fiber optic bundle[31]. Considering that principles for human vision and ordinary photography are based on diffuse reflectance, it is remarkable that diffuse reflectance has not been exploited in the design of imaging optodes. Instrument requirements for an imaging optode based on diffuse reflectance are about the same as for phase ratiometric sensing (Figure 13).

Evanescent wave spectroscopy

Compared to diffuse reflectance, evanescent wave spectroscopy and surface plasmon resonance (SPR) are based on internal rather than external reflections. When light passes from a material with a high refractive index into a material with low refractive index a proportion of the incident light is reflected from the interface, while the remaining fraction is transmitted according to Snell's law (Figure 5c).

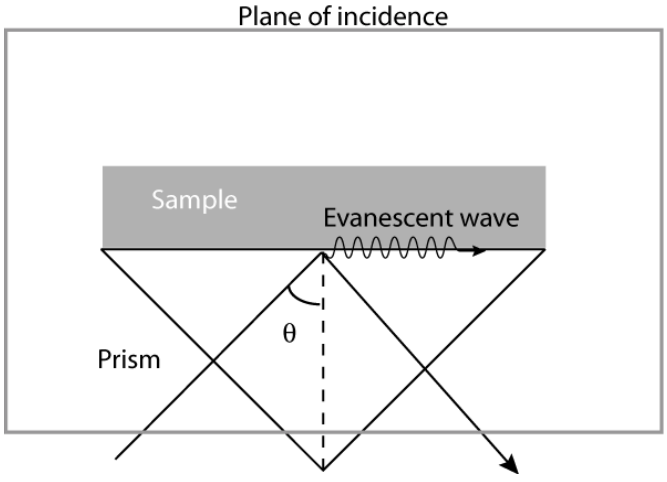

Figure 6. Optical setup for evanescence field measurements.

The refracted ray bends to the surface as the angle of incidence (θ) becomes greater[17]. At the critical angle (θ_c), the refracted wave is completely submerged at the interface. When the angle of incidence is greater than the critical angle, the light is completely reflected (total internal reflection)[17]. However, a new wave, the evanescent wave[32], propagates along the surface and decays exponentially in the direction of an outward normal to the boundary (Figure 6). Typically, the depth of penetration into the media of the lower refraction index ranges from ~50 to ~ 1200 nm depending on the wavelength of the incident light, the refractive indices of the two media and the angle of incidence[28] (Eq. 5). Thus, the evanescent field is absorbed or scattered in the close vicinity of the surface. However, the light field can also be utilized to excite fluorophores in this region and thereby be included in the design of optical sensors. Evanescent wave spectroscopy has been applied on FOCS where part of the cladding has been removed and replaced by molecules sensitive to the analyte. For oxygen determination, the evanescent field at the surface of an optical fiber was used to excite a fluorescent ruthenium complex (Ru(II)tris(4,7-diphenyl-1,10- phenanthroline)) trapped in a sol-gel matrix[33]. The same optical setup was also used to determine pH by incorporation of bromophenol blue in the sol-gel matrix. However, in the latter case, the sensing scheme was based on light absorption[33]. The instrument required for imaging resembles that for surface plasmon resonance imaging (SPRI) in the following section (Figure 10) but without the interfacial metal film. Drawbacks using evanescent field for detection of solutes include that changes in the refractive index due to the analyte or other compounds also alter depth of light penetration, which affect the reflected angular light intensities. The sample background is normally a considerable problem in most imaging techniques and even fluorescence lifetime measurements utilizing transparent optode films have experienced drawbacks associated with sample background[34]. To exclude background effects, an optical isolation between the sample and optode film is therefore often used. However, this procedure makes it difficult by visual inspection to relate the analyte concentration to the imaged object. The main benefit of using evanescent field for excitation of imaging optodes is that it can be used in combination with completely transparent optode films without effects from backscattered or reflected luminescence associated with the studied object. The proposed setup (Figure 7; Strömberg unpublished) might find use in optodes based of fluorescence properties.

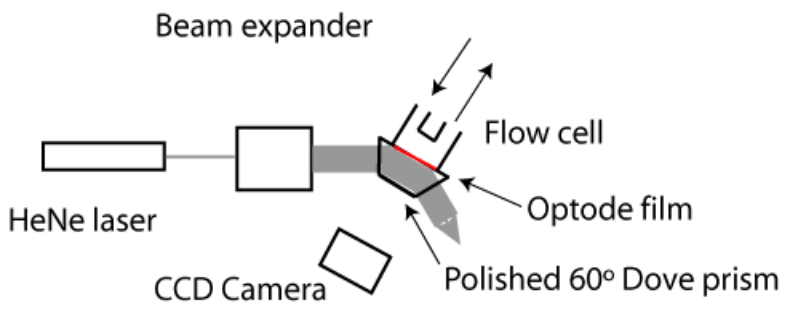

Figure 7. Proposed setup for evanescence wave excitation suitable for imaging fluorescence optodes to avoid background scattering from the sample.

$$\frac{\lambda}{d_p} = 2\pi n_1 \left[\sin^2\theta - \left(\frac{n_2}{n_1} \right)^2 \right]^{\frac{1}{2}} \qquad \text{(Eq. 5)}$$

λ	wavelength
d_p	depth of penetration
n_1	refractive index dense media
n_2	refractive index rare media
θ	reflection angle

Surface plasmon resonance (SPR)

Some of the drawbacks associated with evanescent wave sensors are, however, utilized in surface plasmon resonance (SPR). In SPR, a thin metal coating, usually gold or silver, is applied on the surface between the high and the low refractive media. The evancent wave vector excites electrons in the metal coating, which results in an oscillation dipole (surface plasmon resonance). Only light with the electric vector parallel to the plane of incidence excite the surface plasmons[35] (Figure 8).

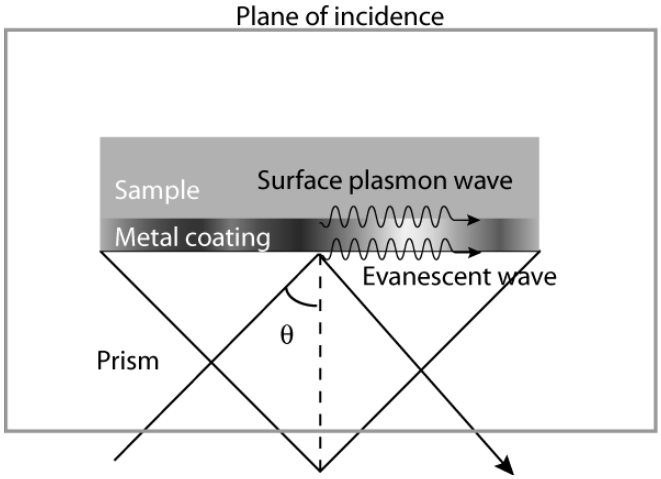

Figure 8. Optical setup for surface plasmon measurements.

Energy loss due to the coupling between the incident light and the surface plasmons reduces the intensity of the reflected light. The intensity of the reflected light reaches a minimum at an angle slightly greater than the critical angle, i.e. the surface plasmon resonance angle (θ_{spr}) (Figure 8). Molecules of a higher refractive index than that of the surrounding media in the evanescent field change the reflected intensity and affects θ_{spr}. Both these effects could be utilized for sensing of analytes. The reflectance value can be obtained by using a ratio of the reflected intensities from vertically and horizontally (parallel and perpendicular to the plane of incidence) polarized excitation light[36].

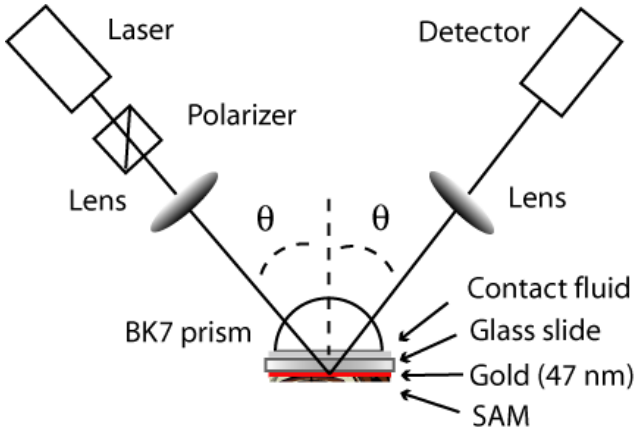

Figure 9. Optical layout for SPR instrument redrawn from reference[37]. The sample is brought into contact with a hemispherical prism in order to couple the laser light with surface plasmons at the gold surface. Rotating the sample and prism assembly allows the reflectivity to be recorded as a function of the incident angle, θ. The setup was used for detection of poly-L-lysine adsorbed onto a self-assembled monolayer (SAM) of 11-mercaptoundecanoic acid formed on the gold substrate.

To create an internal reflection, light needs to propagate from a dense media to a rare media, i.e. the opposite situation as for diffuse reflectance. Normally SPR instruments fulfill this requirement by a hemispherical prism or an equilateral triangular prism[37] (Figure 8, 9). Ruled gratings have also been utilized. However, such gratings could not easily be integrated in the design for imaging optodes as the film is illuminated on one side and the plasmons face the sample on the other side. Angular and wavelength modulations are the most frequently used methods in SPR to measure the change of refraction index caused by analytes[38]. In angular modulation, a converging beam of light is launched into a prism where rays strike the metal film in many different angles simultaneously. The coupling produces a narrow dip in the angular spectrum of the reflected light that is detected with a position sensitive photo detector (CCD or diode array). Wavelength-modulation based SPR- sensors use a collimated beam of white light to induce resonance at the surface. A spectral dip is observed using a spectrograph corresponding to the refractive index change.

Full-frame surface plasmon imaging (SPRI) has so far been based on detecting the change of monochromatic intensities when exposed to an analyte rather than a change in angle[39,40]. The proposed setup for surface plasmon imaging include illumination, equilateral prism and CCD detector (Figure 10).

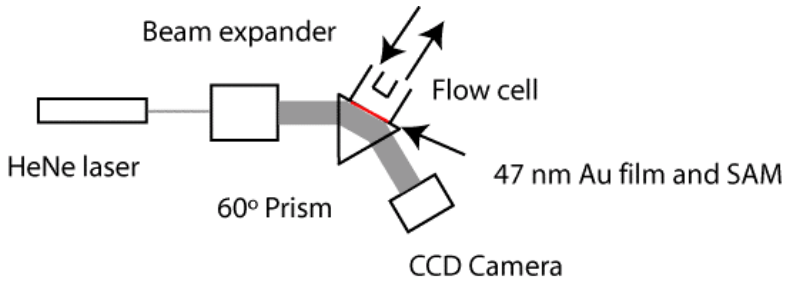

Figure 10. Optical setup for surface plasmon imaging (SPRI) redrawn from reference[40]. A HeNe laser beam is sent through a beam expander, which is required to illuminate the entire sample surface. The expanded beam is directed at the prism sample assembly. A 47 nm thick gold film on a glass slide was used as a sample substrate for a self assembled monolayer (SAM) film. The prism is needed for total internal reflection to create an evanescent wave that couples to the electrons in the gold film. The reflected intensity from the gold film at a fixed SPR- angle was detected with a CCD.

SPR has been widely used for studies of biomolecular interactions and quantification of analytes. The main advantage of SPR is the ability to detect molecular interactions without using radioactive or fluorescent labels. In addition, analytes do not need specific characteristics such as fluorescence absorption or scattering. The main requirement for detection is that analytes induce a change in refractive index when interacting with the metal coating. However, if absorbing molecules appear in the region of the evanescent wave, a reduction in reflectance will follow. An extensive theoretical study of absorption-based SPR has been described[41] as well as experimentally tested for sensing of sodium ions[36]. The main limitation of SPR sensors is the selectivity to the analyte, which is solely based on the ability of the biomolecular coating to recognize and capture the target analyte molecules while preventing other molecules from adsorbing on the surface[38]. A reverse problem is that many substrates possess an extreme affinity for the analyte. This would cause the SPR-chip to lose its sensor characteristics[38]. In those cases, the chip needs to be rinsed or annealed to decouple the analyte. The best commercial SPR-systems are able to detect analytes within a relatively large size range, from relatively small (~ 200 daltons) to medium sized (~ 30 000 dalton) compounds at concentrations below 1 ng/ml[38]. Large proteins cause a major part of the analyte to be outside the evanescent wave and therefore less efficiently detected. Since SPR is based on refractive index changes caused by the analyte it is remarkable that small molecules such as NO_2 (g)[42], H_2 (g)[43], aldehydes and alcohols[44] have been detected using SPR.

A possible drawback with the sensing scheme is the decomposition of the analyte specific coating on the SPR chip and the lack of a normalization procedure that could be used to compensate for this loss over time. During detection of hydrogen gas, the repeated adsorption and desorption of the analyte caused a significant drift in sensor response over time[43]. Even though the drift was greatly reduced by a nickel/palladium alloy as SPR substrate instead of pure palladium, the technique would generally benefit from a drift compensation procedure to accomplish accurate measurements over extended time periods.

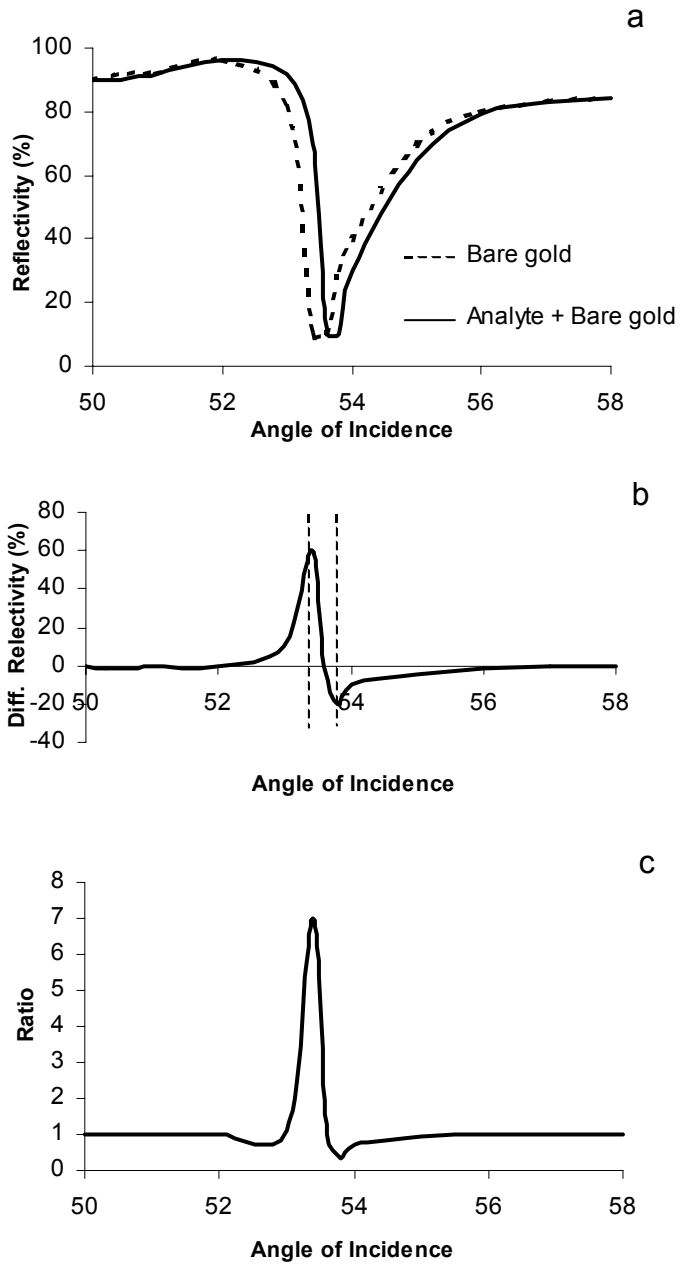

Figure 11. SPR curves illustrating the angular shift due to analyte binding to the substrate (a) (modified and recalculated from reference[45]). A differential SPR reflectivity curve obtained by substracting the two curves in a. A ratio of the two curves in a (not performed in reference). The dashed lines indicate possible angle settings for a SPR ratiometric measurement.

A light-scan at different angles of incidence on bare gold and substrate-coated gold, respectively, could be used to determine the optimal excitation angle in a sensing application (Figure 11a). Subtraction of these scans results in a differential reflectivity curve with two peaks indicating the optimal angles of incidence for imaging[45] (Figure 11b). The maximum and minimum values represent the angles of maximum contrast in an image. The SPR curves (Figure 11a,b) reveal a similar response pattern as obtained for the dual excitation and emission ratio used in the ammonium sensor for intensity normalization (Paper II). Thus, maximum and minimum values could (at

least theoretically) be used in a reflectivity ratio to remove uneven illumination, variations of the sensitivity due to uneven coverage of the analyte recognition coating and minimize the effect of decomposition over time. By using the intensity captured at optimal angle settings in a ratio (53,4°/53,8°), represented by the dashed lines in the differential reflectivity curve (Figure 11b), the absolute signal is amplified from 0.33 to 7 after exposure to the analyte, i.e by 2100 %. The ratio of the curves in Figure 11a, shows the tremendous signal amplification which is mainly due to the sharp dips associated with SPR (Figure 11c). Thus, the feasibility of ratiometric approaches in SPR should be thoroughly tested and evaluated. SPR ratiometric imaging could be achieved by either excite the sample at two different angles or modify two wavelengths to a corresponding angle setting.

Luminescence

Fluorescence and fluorescence quenching

The most widely used sensing scheme for imaging optodes is based on fluorescence intensity either directly, or inversely (quenching) proportional to solute concentrations. The first imaging optode was made for oxygen by measuring fluorescence intensities from the sensing film. The ability to quench fluorescence and phosphorescence was discovered in 1935 by Kautski and Hirsch[46]. They studied quenching effects of surface-adsorbed dyes such as trypoflavin, benzoflavin, safranin, chlorofyll, phorphyrines and others triggered by oxygen. This study initiated developments towards the first optode in 1968[16]. Other studies of poly-aromatic hydrocarbons have been reported, of which pyrene or pyrene-derivatives seem to be the most investigated[47-51]. Today, optical sensing of oxygen basically relies on fluorescence quenching of various quantum efficient ruthenium complexes incorporated in silicone[52-55]. Ethyl cellulose, polyvinylchloride and cellulose acetate buturate are additional polymers that also have been investigated as polymer matrix in oxygen optodes[56]. Silicone rubber as well as PVC are used due to their excellent gas permeability, while being relatively impermeable to ions[53]. The sensor is thereby more or less insensitive to quenching from molecules containing heavy atoms like iodine and bromine[53], that promote intersystem crossing[25]. Major difficulties with this type of sensor are associated with the immobilization technique used to distribute the dye homogeneously in the silicon rubber. As ruthenium complexes are nearly insoluble in silicone, more or less complicated and sophisticated immobilization techniques have to be used[52-55].

Fluorescence intensity is reduced by a wide variety of processes, e.g. fluorescence quenching. The sensing mechanism relies on dynamic quenching by oxygen of fluorescent dyes with a long (~µs-ms) fluorescence lifetime. Quenching associated with oxygen can be caused by oxidation of the dye, formation of non-fluorescent complexes[7] (static quenching) or more commonly, by the paramagnetic behavior of the oxygen molecule[7]. During interactions between the dye and a paramagnetic quenching molecule, fluorescence is either deactivated to the ground state, or transferred via intersystem crossing to the triplet state[25].

Collisional quenching can be described by the Stern-Volmer equation (Eq. 6). Heavy atoms, halogens, amines and electron deficient molecules are also known to quench fluorescence, the former due to the heavy atom effect[7,25]. Quenching can also occur due to absorption of the dye itself, or other absorbing species, i.e. inner filter effects (Eq. 2).

$$\frac{F_0}{F} = 1 + K[Q] = 1 + k_q \tau_0 [Q] \qquad \text{(Eq. 6)}$$

F_0 fluorescence in absence of quencher
F fluorescence in presence of quencher
K_q bimolecular quenching constant
τ_0 fluorophore lifetime in absence of quencher
K dynamic konstant
Q concentration of quencher

The general principle of fluorescence imaging optodes is to immobilize solute specific fluorescent dyes onto/within thin-layered plastic films. The sensor film in contact with the sample is illuminated at specific wavelengths and images of the fluorescence intensities captured with a camera (Figure 13).

The main drawback with intensity based sensing is that quantification of analytes becomes unreliable due to uneven illumination and dye distribution, as well as changes in the excitation light source. However, the sensor design can without modifications be used for lifetime-based measurements. Today, intensity based imaging of oxygen concentration is out-competed by fluorescence lifetime measurements.

Fluorescence resonance energy transfer (FRET)

The transfer of energy from the excited-state of a donor molecule to an acceptor molecule is referred to as fluorescence resonance energy transfer (FRET)[7]. A certain spectral overlap between the emission spectrum of the donor and absorption spectrum of the acceptor is required for the energy transfer process. Fluorescence energy transfer is distinguished from re-absorption in that no photons are involved in the process. The transfer is caused by dipole-dipole interactions between the donor and acceptor molecule typically separated 20-60 Å apart. The rate of energy transfer is inversely proportional to r^6 (r = distance between the molecules)[7]. The concept has been widely used for distance measurement between two sites of a macromolecule. In addition, it has been utilized for studies of protein-protein interactions[57,58]. However it also constitutes a suitable sensing scheme for detection of analytes due to normalization of fluorescence intensities. Upon binding to the analyte, the fluorescence subsequent to excitation of the donor molecule is quenched due to the energy transfer to the acceptor molecule that displays fluorescence. Subsequent excitation of the donor dye, a ratio of the donor and the acceptor fluorescence intensities is used for quantification of the analyte. FRET has been used for detection

of lead (II) ions[59], potassium[60] and hydrogen ions[61]. For potassium the conformational change due to the binding of the analyte causes the donor to approach the acceptor, which causes FRET. The technique facilitated ratiometric detection of potassium at submicromolar levels under optimal conditions and the selectivity for potassium against sodium was 43000 times i.e. highest ever reported. Quantum dots have also been utilized in a FRET design for detection of maltose[62]. Quantum dots are extremely photo stabile nano crystals of semiconductor materials (CdSe or CdTe)[62] that have a broadband excitation and narrow emission (~25-45 nm) that span over the visible spectrum. Instrument requirements for an imaging optode based on FRET are about the same as for phase ratiometric sensing (Figure 13).

Wavelength ratiometric sensing scheme

Among the drawbacks with intensity based fluorosensors are the limited long-term stability due to photobleaching and wash-out of the dye[7]. In principle, part of the problems encountered with intensity based fluorescence sensing can be avoided using fluorophores that display spectral changes in the absorption and/or emission spectra upon binding or interacting with the analyte, i.e. wavelength ratiometric dyes [7]. In a ratiometric sensing scheme, the fluorescence intensity following excitation at two excitation wavelengths (alternatively, one excitation and two emission wavelengths) is normalized by a quotient. This procedure ideally cancel out variations in fluorescence intensity not related to analyte concentrations but rather to changes in e.g. excitation light intensity and effective concentration of the indicator dye[63]. The pH sensitive organic acid hydroxypyrentrisulfonic acid (HPTS), and the calcium indicators Fura-2 and Indo-1 are examples of wavelength ratiometric probes that are successfully used in clinical and environmental sciences[26,64,65]. Wavelength ratiometric dyes are based on intramolecular charge transfer[66]. When a fluorophore contains an electron-donating group (often an amino group) conjugated to an electron-withdrawing group, it undergoes charge transfer from the donor to the acceptor upon excitation by light. If the electron-rich terminal of the fluorophore interacts with a cation, the absorption spectra is blue shifted. One of the main drawbacks associated with wavelength ratiometric dyes is the limited number of dyes that are solute specific and ratiometric. After about 20 years of development, wavelength ratiometric dyes are only available[66] for H^+, Ca^{2+}, Na^+, Mg^{2+} and Zn^{2+}.

The instrumental setup for imaging is the same as for phase ratiometric sensors (Figure 13). However, the interference filters could have a wider bandpass or be completely replaced by longpass filters.

Imaging optodes using a ratiometric sensing scheme has been utilized for screening of pH variations in sediments. The first imaging optode for pH was introduced 2002, based on HPTS directly adsorbed on specific transparency-films[65]. The concept was further improved by covalent immobilization of HPTS to poly(vinyl alcohol)[67]. The optode retained its original properties after continuous exposure to natural marine sediments for two months. In this latter case, an inexpensive (~ 800 $) commercial

digital single-lens reflex camera (Canon EOS 10D) and light emitting diodes were employed for detection.

Phase ratiometric sensing scheme

The development of new selective and ratiometric dyes is cumbersome which has caused a limited analyte palette. Therefore, additional and complementary approaches are required to facilitate selective fluorescence detection of analytes. The significant focus on ionophore-based optodes is probably caused by the large amount of highly selective ionophores developed and used in ion-selective electrodes. Thus, by finding a single self-referenced sensing scheme, numerous of analytes could most likely be optically detected in a similar fashion by replacing the ionophore. The idea to selectively utilize an ionophore-mediated phase transfer of the analyte together with a dye (coextraction), was originally introduced in 1977[68]. The coextraction technique was used to measure potassium in blood serum. Until 1999, the concept was progressively improved by utilizing coextraction of potassium and a solvent sensitive dye in a hydrogel ether emulsion[69]. The rather unusual sensor configuration increases the interfacial area, whereby sensitivity as well as response time are improved compared to multilayered two-phase films[70]. An ionophore is used to selectively mediate the phase transfer of the analyte. The ability of an indicator to change its spectral properties with the polarity of the surrounding medium is called solvatochromism[69,71], a property associated with the chemical structure of the dye. Solvatochromic indicators often have a polar and a nonpolar part, which give them a typical detergent structure. By a proper choice of the hydrophilic to lipophilic balance of the dye, no additional blocking layer is required to prevent leaking of the dye[69,71]. Only dyes with $K_1 >> 1 > K_2$ are useful in sensing applications (Eq. 7). This relation illustrates no leaking of the dye to the surrounding solution and no dye completely submerged in the organic phase in absence of the analyte. Due to the detergent structure dye molecules are most likely associated with the hydrophobic phase and the position is altered due to the coextraction process (Figure 12).

Exposure to the analyte induces a reversible wavelength shift in fluorescence of about 20 nm together and increases overall fluorescence intensity. Large efforts have been made to make these systems self-referenced but basically all of them include addition of an inert reference dye[6,72]. In 2003, we made use of a ratio representing the dye molecule in either phase, i.e. a phase ratiometric sensing scheme (Paper II). A similar concept has previously been reported for determination of membrane potential and intra – membrane electric fields in lipid vesicles and in cells[73,74].

The coextraction, or ion pair extraction technique differs from the more traditional process of ion exchange in that two ions of opposite charge are extracted simultaneously, rather than a complete replacement. In most sensors based on ion exchange, deprotonation of a dye results in a fluorescence shift. Electro-neutrality is maintained in both techniques. However, while the ion exchange mechanism is highly pH dependent, coextraction is pH independent.

$$D_S \xleftrightarrow{K_1} D_H \xleftrightarrow{K_2} D_L \qquad \text{(Eq. 7)}$$

D_s dye concentration in solution
D_H dye concentration in hydrogel
D_L dye concentration in 2-(Dodecyloxy)benzonitrile
K_1 partitioning constant solution/hydrogel
K_2 partitioning constant hydrogel/2-(Dodecyloxy)benzonitrile

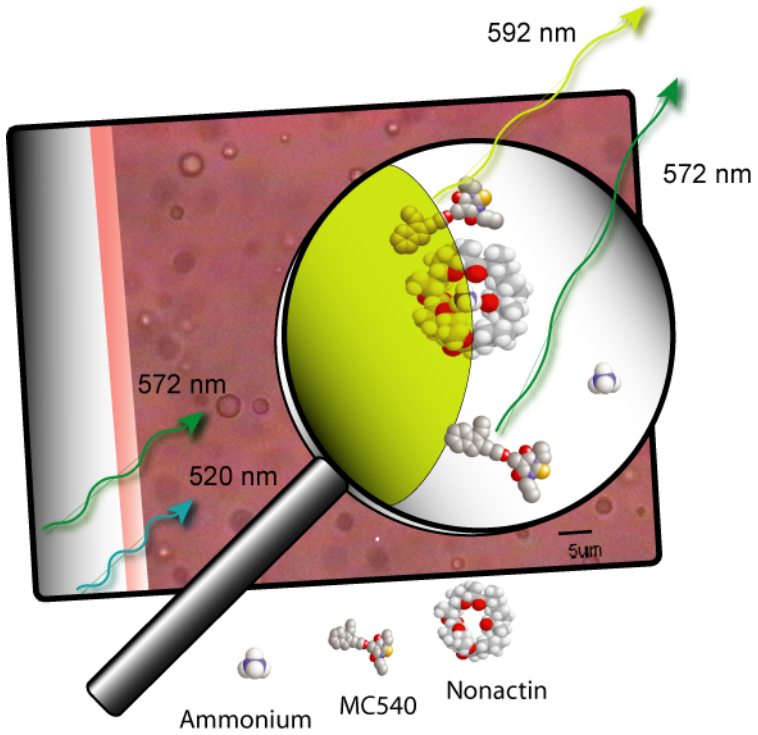

Figure 12. The solvatochromic Merocyanine 540 (MC 540) used for detection of ammonium (Paper I-V) has a large Stokes´ shift and magnifies the signal about 100 times in 2-(Dodecyloxy)benzonitrile compared to in hydrogel (31, 32). The excitation/emission maxima of MC 540 in the 2-(Dodecyloxy)benzonitrile ether droplets were shifted to 572/592 nm, while the exitation/emission maxima in the hydogel were 520/572 nm.

Interference filters with a small bandpass (2 nm) are normally required to resolve the small shift in fluorescence associated with the phase transfer. However, the light transmission of bandpass interference filters is dependent on the angle of the incident light. Preferably, the incident light should be orthogonal to the surface of the filter and the optical system therefore have infinity-corrected optics (Figure 13).

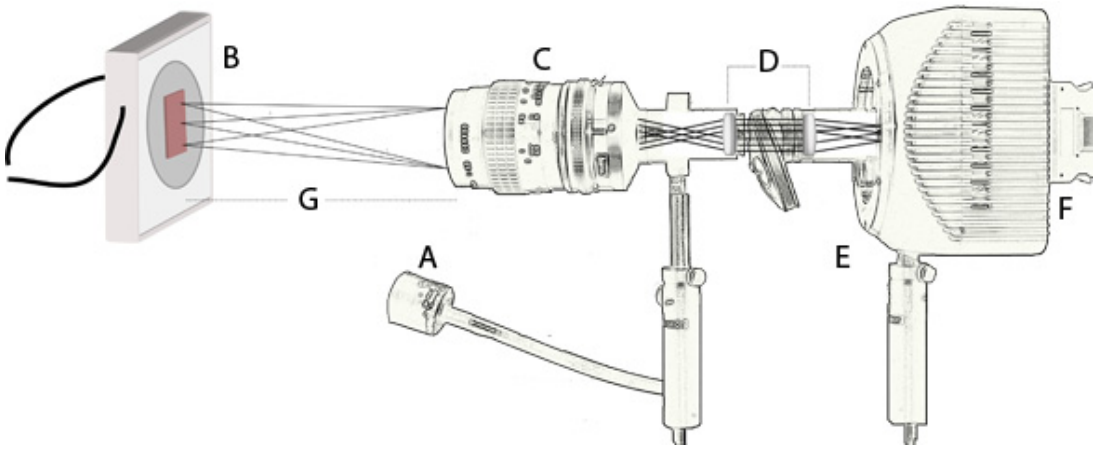

Figure 13. The optical system and flow through cell. The illustration describes the excitation focusing lens (A); the flow through cell with applied sensor (B); the macro lens (C); the infinity region with bandpass filters for wavelength selection (D); the CCD camera (E); the image data transfer to computer (F) and the object distance and angle of excitation was 30 cm and 30°, respectively (G).

The new ratiometric concept for optodes was found to cancel out uneven illumination and variations in the excitation light source (Paper II). Moreover, it was found to cancel out pH changes (Paper II) as well as reduce sensor drift over time (Paper III). Mainly due to the short fluorescence lifetime associated with Merocyanine 540 (MC540), the response is also independent of oxygen, a well-known quencher of fluorescence. Surprisingly, the ratiometric normalization did not compensate for uneven dye distributions (Paper II). High concentrations of MC 540 cause build up non-fluorescent dimers[75], which displaces the ratiometric protocol. If background subtraction is performed this effect will be eliminated, however, background subtraction invokes other problems (see next section) and was therefore avoided.

Anisotropy

When a fluorescent molecule is illuminated with polarized light, the electrons move in a preferential direction described by the direction of the transition moment for absorption. Molecules with the absorption transition moment aligned parallel to the electric vector of the polarized light have the highest probability to be excited. Orientations deviating form this condition give a reduced absorption efficiency. Under specific circumstances, the fluorescence emission is also polarized, usually expressed in terms of anisotropy (Eq. 8) or polarization. Depolarization of the emission is most often caused by rotation during the excited state. The size and shape of the rotating unit, as well as the viscosity of the solvent, influence the rotation speed and thus the anisotropy[7]. The simplest model of depolarization of a single exponential decay, i.e. only one fluorescence lifetime is associated with the sample, is described by the Perrin equation (Eq. 9) assuming a globular rotating unit. A change in rotation motion, molecular size or fluorescence lifetime caused by the analyte can be utilized for sensing.

$$r = \frac{I_{VV} - I_{VH}}{I_{VV} + 2I_{VH}} \qquad \text{(Eq. 8)}$$

$$r = \frac{r_0}{1 + (\tau / \phi_c)} \qquad \text{(Eq. 9)}$$

I_{VV} vertically polarized emission intensity after vertically polarized excitation,
I_{VH} horizontal polarized emission intensity after vertical polarized excitation,
r fluorescence anisotropy
r_0 anisotropy without rotation (ordinarily 0.4)
τ fluorescence lifetime
ϕ_c correlation time

Largest changes in anisotropies upon binding to the analyte are obtained by "tagging" a fluorophore to the rotating unit. The flurophore should have a lifetime of about the same magnitude as the correlation time of the rotating unit[76]. The maximum anisotropy for an isotropic solution is 0.4[7], but dye molecules trapped in stretched polymer films could reach anisotropies close to 0.9[77]. The anisotropy is also close to 1 in the presence of scattering particles, which is commonly utilized for alignment of polarizers[7].

Fluorescence anisotropy has been used in combination with biosensors for the detection of picomolar concentrations of metal ions such as Cu (II), Co (II) and Zn (II)[76]. In essence, the correlation time of carbonic anhydrase (~15 ns) was matched with the lifetime of sulfonamidobenzoxadiazole (12.1 ns) to yield highest possible changes in anisotropy. The fluorescence intensity was quenched subsequent to the addition of Co (II) or Cu (II), which also caused a reduced fluorescent lifetime. Thereby the anisotropy increased. However, since Zn (II) is not a notably effective quencher of fluorescence[76], the active site of the carbonic anhydrase was labeled with a moderately solvent sensitive probe that upon binding to Zn (II) reduced its mobility (affecting the correlation time ϕ_c) which increased the anisotropy.

Imaging optodes for Cu (II), Co (II), and Zn (II) can be designed by incorporating carbonic anhydrase variants labeled with derivates of benzoxadiazole sulfonamide in a hydrogel matrix with high water content. However, the matrix will probably increase the rotational correlation time (ϕ_c). Choosing a dye with slightly longer fluorescent lifetime to maximize changes in anisotropy could compensate for this drawback.

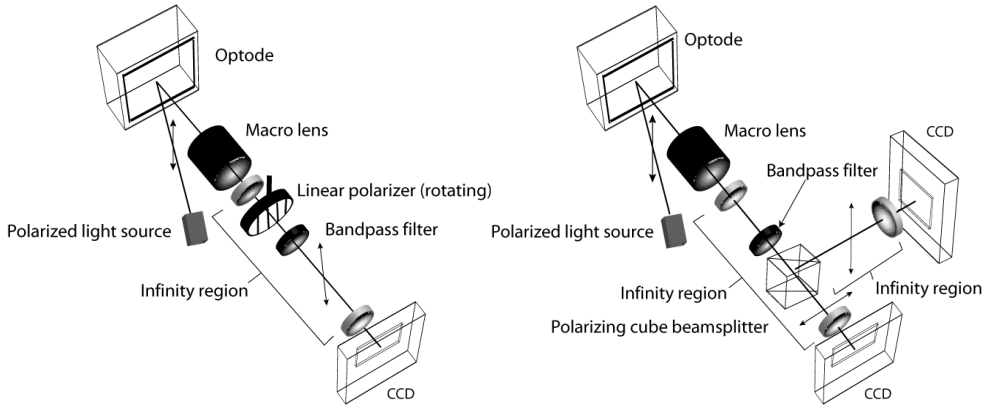

Figure 14. Proposed optical setups for imaging anisotropies from optodes with dual and single detectors.

Ideally, two detectors are used for anisotropy measurements to comprise both vertically and horizontally polarized emissions at the same time. Fluctuations in excitation light intensity are likely efficiently cancelled out (Figure 14) Two detectors might on the other hand cause individual sensitivity changes between the detectors. An alternative to dual detectors is to switch a polarization filter ahead of a single detector, similar to the principles employed for ratiometric sensing (Figure 14). An interesting instrumental setup with one detector but without any moving parts has been used for imaging single molecule anisotropy. Lateral and rotational diffusion of fluorescent-labeled lipids on supported phospholipids membranes[78] were simultaneously detected. The instrument made use of a polarizing beam splitter (Wollaston prism polarizer) that separated horizontal and vertically polarized light before reaching the CCD (Figure 15.). Two different regions of the CCD represent the polarization-separated images used for calculation of the anisotropy in each pixel.

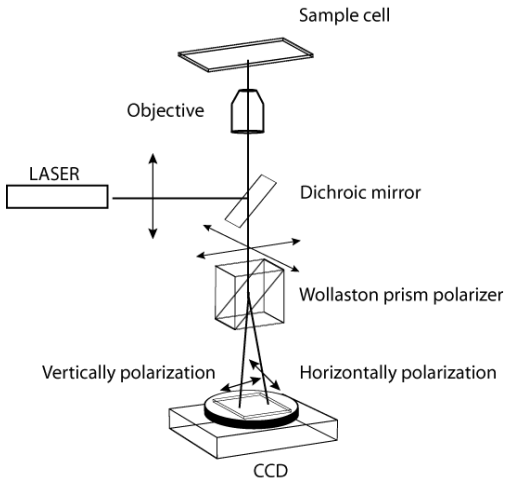

Figure 15. Experimental setup for anisotropy imaging using an inverted microscope setup. Redrawn from reference[78].

Anisotropy measurements are inherently ratiometric and thereby independent of fluorophore concentration and excitation light intensity as long as measurements are not distorted by autofluorescence, scattering and a poor signal to noise ratio. Measurements of anisotropy in solution are limited to samples free from scattering particles since they produce polarized light[17] and thereby disturb the anisotropy of the analyte signal. The effect from scattering is probably minimized when the sensing molecules are confined in a polymer matrix. However, molecular sieves that exclude compounds of certain cut-off molecular weight could be utilized as backing for the optode. Thereby fluorescence and scattering from molecules larger than the analyte are excluded. A major disadvantage seems to be the limited long-term stability of the proteins used for biosensing. For example, denaturation of the proteins caused the sensor used for determination of Cu (II) in seawater to loose about 50% of the response after 4 hours of measurements[79]. Such a large loss in intensity most likely also reduce the signal to noise relation and thereby the sensitivity of measurements over time. An alternative to the highly selective proteins could be to synthesize rigid substrates tagged with fluorophores of a comparable lifetime of the rotational correlation time. However, the selectivity to the analyte associated with natural proteins found in nature rivals most (if not all) sensing systems made by man.

Fluorescence lifetime (frequency and time domain)

Fluorescence lifetime is the average time the fluorophore spend in the excited state following excitation[80]. After a short pulse of light, a fraction of the fluorophores will be in the excited state. Depopulation from this state proceeds through non-radiative relaxation processes and by emission of fluorescence[7]. Thus, the overall relaxation to the ground state is expressed by Eq. 10.

$$\frac{dn(t)}{dt} = -(\Gamma + k_{nr})n(t) \qquad \text{(Eq. 10)}$$

$n(t)$	number of excited fluorophores at time t
Γ	emissive rate
k_{nr}	non-radiative decay rate

Depopulation causes the observed intensity to decay in an exponential fashion. Many fluorophores have single exponential decays[81], i.e. only one emissive rate is associated with the fluorophore (Eq. 11). If a mixture of fluorophores are excited simultaneously, or the fluorophore is associated with more than one emissive rate, the intensity decay becomes complex and multi-exponential (Eq.12).

$$I(t) = I_0 e^{\left(\frac{-t}{\tau}\right)} \qquad \text{(Eq. 11)}$$

$$I(t) = \sum_i \alpha_i e^{\left(\frac{-t}{\tau_i}\right)} \qquad \text{(Eq. 12)}$$

$I(t)$	fluorescence intensity at time t
I_0	fluorescence intensity at time zero
t	time
τ	lifetime
α	amplitude or intensity for each component at time zero for multiexponential decay

The inverse of the emissive rate is called the intrinsic or radiative lifetime, which is usually longer than the measured lifetime due to intermolecular processes and intermolecular interactions[80]. Dynamic quenching, energy transfer, solvent relaxation and analyte binding affect the fluorescence lifetime and could be utilized in sensing schemes for analyte detection.

Frequency- and time-domain measurements are two complementary techniques to determine the fluorescence lifetime. In the time domain, the sample is illuminated with a pulsed light. The pulse time is preferably much shorter than the decay time of the sample. A time-gated detector captures the following fluorescence from each light pulse at different times after excitation. However, if the sample has a single exponential decay, two time-separated measurements are sufficient to calculate the lifetime. The decay time of the sample is usually calculated from the slope ($-1/\tau$) of the logarithmic intensity versus time (Figure 16).

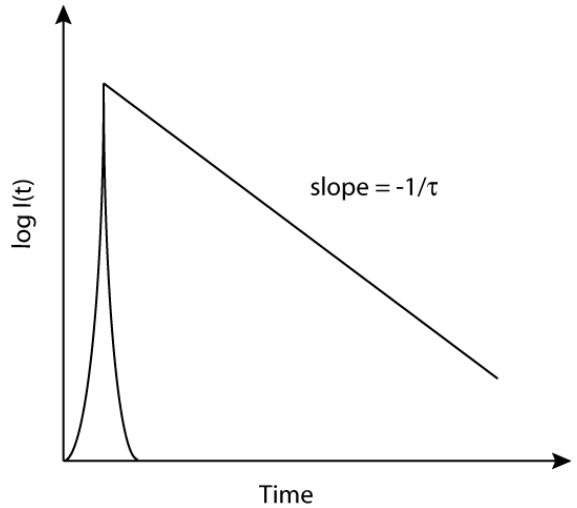

Figure 16. The principle of retrieval of the lifetime from a logarithmic intensity versus time plot.

In the frequency domain, the sample is illuminated with intensity-modulated light. Usually, the amplitude of the excitation intensity is altered with a sine wave of a frequency close to the reciprocal lifetime of the molecule. The subsequent fluorescence is shifted in phase due to the lifetime of the fluorophore. The shape of the sine wave of the fluorescence might also be distorted due to emission when the

excitation is at minimum. This effect (demodulation) can in addition to the phase shift (phase angle) be utilized for determination of the fluorescence lifetime (Eq. 14).

$$\tau_\phi = \omega^{-1} \tan\phi \qquad \text{(Eq. 13)}$$

$$\tau_m = \frac{1}{\omega}\left[\frac{1}{m^2} - 1\right]^{\frac{1}{2}} \qquad \text{(Eq. 14)}$$

$$m = \frac{B \times a}{A \times b} \qquad \text{(Eq. 15)}$$

τ_ϕ	lifetime using phase shift
ω	angular temporal frequency (2π×frequency in hertz)
ϕ	phase angle (radians)
τ_m	lifetime using modulation
m	modulation
a	average excitation intensity
b	modulated amplitude; excitation light
A	average emission intensity
B	modulated amplitude; emission light

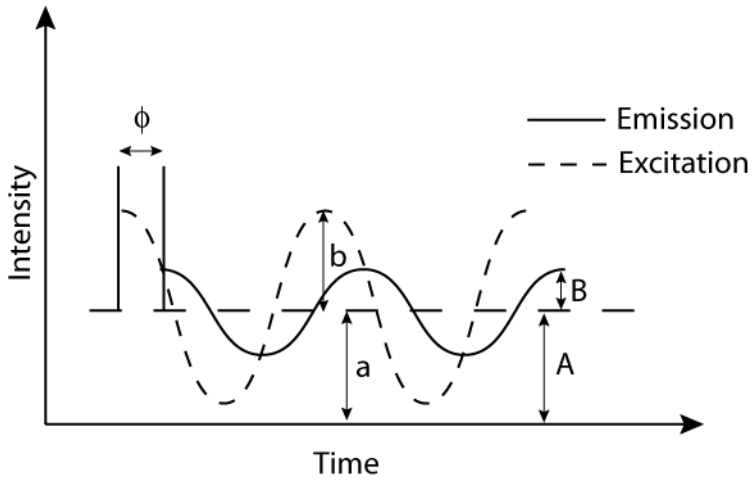

Figure 17. Phase modulation

Fluorescence lifetime imaging (FLIM)

Commercial instruments are available for fluorescence lifetime in the time and frequency domain, respectively. Key components in these systems include the multi-channel plate and light-modulation unit. The difference between these techniques is found in the pulse generator producing either a sine wave or a short finite square pulse. Thus, both frequency and time domain measurements should be possible to perform with basically identical instrumentation. Two instrumental configurations are briefly described below.

A typical frequency domain instrument is based on the modulation of the sensitivity of the intensifier (based on multi-channel plate) by the same frequency as the light source (LED) but with an adjustable phase shift. The detector signal depends on the

phase-shift of the fluorescence signal relative to the modulated sensitivity of the detector. Several images are captured representing different phase shifts at the detector. A sine-wave is fitted through each pixel from a stack of images ordered after increasing phase angle. The lifetime is calculated from the modulation depth or the phase shift relative the excitation light according to Eq. 13 and Eq. 14, respectively.

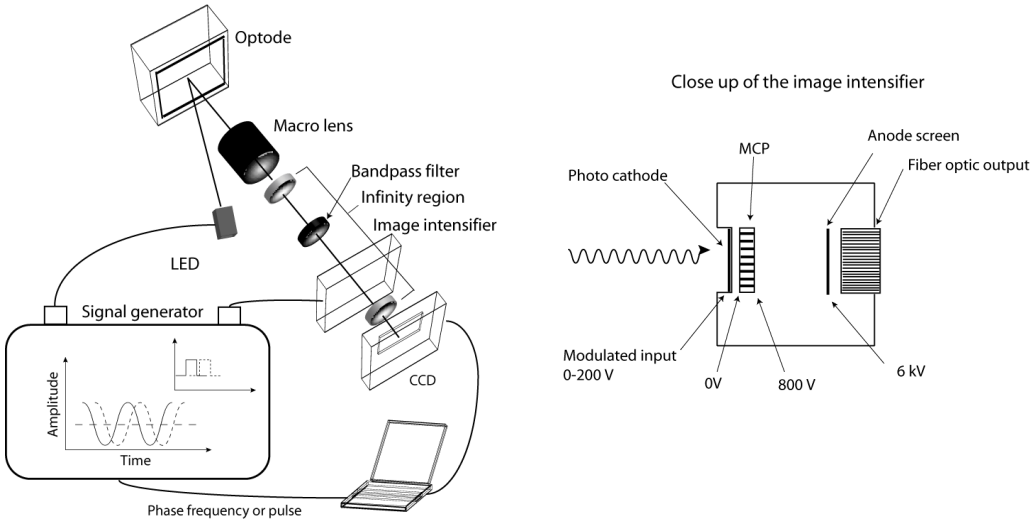

Figure 18. Proposed infinity corrected FLIM setup comprising both frequency and time domain measurements. The LED light source emits unpolarized light, however, if a polarized light source is used for excitation, a polarizer deviating 54.7° (magic angle) from the excitation polarization must be included in the infinity region. A magic angle condition is used to avoid anisotropy and/or rotational diffusion effects on the intensity decay subsequent excitation with polarized light.

In a corresponding time domain instrument for imaging, the fluorescent sample is illuminated by a short pulses (~ 10 ps), at a high repetition rate (~ 5 kHz). Images are captured using a fast-gated image intensifier (~110 ps). The intensifier is triggered by a simultaneous pulse from the excitation light source that could be digitally delayed for different lifetimes. Several images are captured at the detector representing time delays following excitation. A least square fit in each pixel of a stack of images ordered in time is used to calculate the fluorescence lifetime.

A modular system without image intensifier has also been developed based on a relatively fast gated CCD camera (500 ns) using the pulse-gate approach in the time domain[34,82]. The large gate width makes the system limited to phosphorescent molecules and thus suitable for oxygen sensing at a much lower price than for the CCDs equipped with image intensifiers. Alternatively, this system could be used with the t-DLR approach described in the next section. Targeted laboratory evaluations and field studies concluded that, owing to high accuracy (+/- 2 μM), long-term stability (more than 20 months), lack of pressure hysteresis, and limited cross-sensitivity, the method was overall more suitable for oxygen monitoring than other methods[83].

Dual lifetime referencing (t-DLR)

An alternative concept to lifetime based imaging that make use of a fluorophore/ phosphor couple for referencing fluorescence intensity was presented in 2001[84]. In dual lifetime referencing (t-DLR), luminescence is recorded both during and after illumination (Figure 19). The short-lived indicator fluorescence and the long-lived phophorescene of the "inert" reference are simultaneously excited and measured in two time gates. In the first time gate emissions from the reference compound and the sensing dye is captured during constant illumination. Following the excitation pulse, only the phosphorescence from the reference is collected in the second time gate, as the fluorescence lifetime of the analyte sensitive dye is too short to be recorded. A ratio of these images ideally results in an image free from artefacts associated with optical interferences like variations in excitation light intensity and uneven illumination of the sample. It needs, however, to be emphasized that spatial proximity and a constant ratio of the fluorescent and phosphorescent dye within the imaged surface are required to make t-DLR scheme accurate. Other objections to this sensing scheme include that the reference needs to be completely inert and the analyte and reference dyes are subjected to different photodecomposition and leakage. The used reference dye also need to be encapsulated in a gas tight polymer, to avoid effects of collisional quenching by oxygen. Thus, the sensing scheme removes variations of the excitation light source, uneven and illumination and possibly uneven distribution of the analyte sensitive dye. The procedure will not, however, minimize drift in response over time[84]. Though, the sensing scheme facilitates imaging using dye sensors that do not have ratiometric properties. The normalisation procedure has so far been used to detect copper (II)[85], seawater salinity[86], chloride[87], pH[84] and nitrate[88]. The nitrate sensor utilizes a similar sensing scheme as that described for ammonium in this thesis (Paper I). However, the phase shift of the potential sensitive dye was not utilized for normalization of the signal. As discussed in paper III, the fluorescent intensity at 572 and 592 nm decreased to about 18 % of the initial intensity, while the phase ratio was 76 % of the initial value after about 10 days. Thus, the ratiometric procedure compensated for most, but not all, of the signal drift observed for the individual wavelengths.

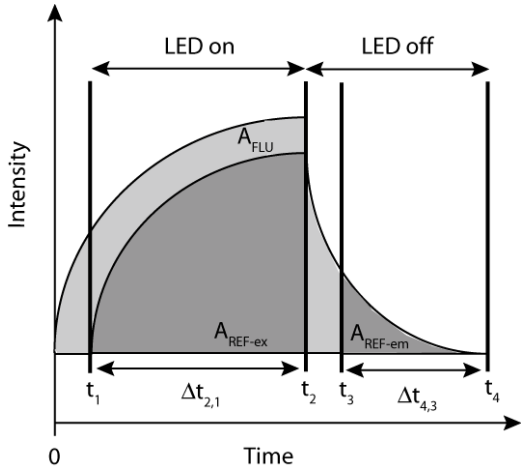

$$R = \frac{A_{ex}}{A_{em}} = \frac{A_{REF-ex} + A_{FLU}}{A_{REF-em}}$$

Figure 19. Principle of t-DLR, redrawn from reference[84]. The image intensity ratio of the intensity images (A_{ex} and A_{em}) captured during $\Delta t_{2,1}$ and $\Delta t_{4,3}$, is denoted as R. The images captured during continuous excitation (LED on) incorporate both intensities from the phosphorescent reference (A_{REF-ex}) and fluorescent dye (A_{FLU}). The denominator in the ratio is only represented by the phosphorescence reference (A_{REF-em}). The time lag between excitation and emission which completely incorporates the fluorescence decay from the fluorescent dye molecule ($\Delta t_{3,2}$) was 100 ns.

As illustrated in this part of the thesis, several detection schemes could be utilized in the design of imaging optodes. However, commercial instrumentation for each detection scheme would become incredible expensive. In addition, instrumentation tends to become hard to adapt to other applications than it was originally designed for. My recommendation is to avoid all commercial software's and instruments when sold in packages. Since most systems rely on basically the same components it is probably better to build your own optical system. Thus, module systems gain in flexibility over commercial instrumentation packages and offer new ways for detection in addition to mixing existing techniques. Finally you are not dependent on instrument specific softwares to process the images.

Data analysis and sensor calibration procedures for imaging optodes

Pixel-by-pixel calibration

Pixel-by-pixel calibration constitutes a suitable and frequently used procedure to calibrate images from imaging optodes. Each pixel is individually calibrated and thereby artifacts like uneven dye distribution and uneven illumination are compensated for. It is important to emphasize, however, that the traditional pixel-by-pixel calibrations neither compensate for fluctuations in the light source nor for variations the optoelectronic system used for imaging. Thus, additional normalization procedures are needed for accurate quantification of the analyte. Many commercial software programs (e.g. NIH, Image J and Incytm) offer calibration through representative average values of the image after exposure to calibration solutions. The concept likely originates from the procedures of ratiometric normalization, which ideally should be "free" from artifacts and thereby independent of individual pixel

responses. Today there is no computational limit for pixel-by-pixel calibrations and since basically all optodes need to be externally calibrated, it is normally advantageous to pixel-calibrate rather than to use a representative mean value of the response for calibration. One of the largest difficulties with pixel-calibration is the required image alignment. Several softwares automatically align images, however, recognition of patterns and matching of the exact position of the image are preferably made by visual inspection. During the experiments presented in Paper III-V, alignments were made using a graphical user interface in Matlab (control point selection tool; cpselect). Control points in the software were aligned manually to fixed points made on the optode substrate, whereafter the software performed magnification and rotation to align the images.

A pixel calibration procedure was used for the first imaging optode. The Stern-Volmer constant and a constant representing non-quenchable fraction of the fluorescence were calculated in each pixel and subsequently used for calibration of the sample images[24]. The pioneering work made by Glud and others resulted in several images of oxygen distributions in an intertidal sediment. The images covered an area of 13×17 mm and correlated well with synchronous oxygen microlectrode profiles in the sediment.

Time correlated pixel-by-pixel calibration (TCPC)

Unfortunately, a significant drift over time not only in fluorescence intensities, but also fluorescence ratio, has been reported. This drawback for sensing applications is, however, barely discussed in scientific articles. One of the few observations described a ~15 % drift in fluorescence ratio of the ratiometric calcium probe Indo-1 following only ten minutes of illumination[89]. The displacement of the fluorescence ratio (Ca^{2+}-bound /Ca^{2+}-free) was attributed to photolysis of the dye to compounds with emission spectra that resembled Ca^{2+}-free fluorescence and was relatively insensitive to Ca^{2+}. In this way, the ratio of free and bound Ca^{2+} fluorescence gradually drifted over time also when exposed to a constant concentration of Ca^{2+}. The ratiometric optode for ammonium presented in this thesis (Paper I-V) drifted about 20% over a ten-day period (Paper III). Observations indicate that also the wavelength ratiometric dye HPTS is associated with a significant drift in fluorescence ratio over time (Haakonen et al, unpublished).

In traditional pixel-by-pixel calibration procedures, each pixel has its own calibration usually retrieved before the experiment. In time-correlated pixel by-pixel calibration, each pixel has its own time dependent calibration function that encompasses calibrations made before and after measurements. This procedure has been found to efficiently compensate for an absolute drift in response, as well as changes in analytical sensitivity over time. The basic idea of this protocol is to link the analyte responses in each pixel from two time-separated calibrations (Paper III). The fluorescence ratios or intensities from the calibrations are linked together by a linear time-dependent function. Concentrations between levels in the calibration at a specific time and pixel are determined by a linear table-look-up interpolation. Thus, the

concentration of the sample is determined at the time of image capture in each pixel using a unique calibration. The calibration curve in each pixel can adapt to various shapes as long as the response is continuously increasing or decreasing with analyte concentration. Thus, analyte response does not have to be linear to be used in this calibration procedure.

The concept can also be utilized to retrieve statistical parameters throughout measurements such as analytical sensitivity, limit of detection and relative signal variation as well as operational lifetime (Paper III-V).

Background subtraction and measurement strategies

Basically all fluorescence intensity measurements are performed by first removing the background caused by the sample without presence of the analyte i.e. blank subtraction. This is also normally performed before normalization in a ratio to avoid different backgrounds at the nominator and denominator wavelengths. However, once background is removed one automatically assumes that the ratio or fluorescence intensity is not drifting. Since signals from many optodes drift over time, background subtractions add additional problems to the measurements. Dark noise subtraction is however always possible during measurements since dark noise is associated with the detector and not with the sample. One way to minimize the problems associated with backgrounds is to initially adjust the intensity levels to approximately the same value at each wavelength used in the ratio and time-correlate the calibration. In Papers III-V a fixed exposure times were used and the calibration curve in each pixel was time correlated.

A completely different approach that minimizes problems with backgrounds is to collect constant fluorescent intensities at both wavelengths close to the dark noise level of the detector (Strömberg et al. unpublished). The acquired time to reach a constant intensity at each wavelength is used for quantification. A problem with this procedure is that commercial spectrofluorometers normally work with fixed integration times and not with fixed intensities. In addition, for finite imaging this technique becomes difficult since each individual pixel could not be shut of when it has reached a specific value. An alternative procedure (Strömberg et al. unpublished) is to fix the denominator wavelength, representing the decreased signal when exposed to the analyte to an approximately constant intensity for most of the pixels in the image over the entire experiment. The integration time (or fixed fraction or multiple of this time) acquired to reach this intensity is used as integration time for the nominator wavelength. This approach facilitates use of the entire dynamic range of the camera. Another benefit is that the camera always operates at a constant low noise level and thus should give approximately the same sensitivity during the operational lifetime of the optode film. The intensity ratio in each pixel could be used for analyte quantification. The operational lifetime of the sensor is now only limited by how long exposure times one could tolerate in a measurement. Eventual drift in ratio is compensated by time correlated pixel-by-pixel calibration and the performance could be tracked over time according to paper IV.

Pixel binning was used to enhance the dynamic range of the imaging sensor (CCD) and ensemble averaging was used in papers III-V to reduce noise and thereby improve the sensitivity of the measurements. The signal-to-noise ratio is proportional to the square root of the number of data collected to determine the ensemble average[25]. Image replication is also used to retrieve the uncertainty of the measurement. However, the fact that sensors measure analytes over time invokes an analytical dilemma. Replication during a change in concentration throughout the measurement will be reflected in the noise between the images. Therefore replication needs to be sufficiently fast in order to reflect the sensor performance and not incorporate the noise associated with a change in sample concentration. Thus, when studying rapidly changing processes, the noise calculated from the replication would both incorporate the chemical and instrumental noise as well as the noise due to a change of the chemistry close to the studied object during the acquired time for image capture. Time correlated pixel-by-pixel calibration was utilized to resolve noise associated with the measuring procedure from the actual noise in the sample (Paper IV). It is important to realize that standard deviations also may say something about the studied process. The relative standard deviation close to the peripheral part of a root structure was compared with the sensor performance retrieved from the TCPC-protocol. The conclusion was that the high relative standard deviation in this region was attributed to fast change in concentration due to the interplay between uptake and supply of ammonium (Paper V).

Conclusions

Some of the spectroscopic techniques and sensing schemes that could be utilized in the design of imaging optodes are exemplified in the introduction of this thesis. Many of them can be used simultaneously or complementary to achieve optimal performance of both the instrument and the optode sensing film. In the following section, I summarize some of the major results obtained during my Ph.D. studies.

In paper I-V, the progressive development and subsequent application of an ammonium imaging optode in natural environments are described. The ammonium optode was unaffected by O_2 concentrations but dependent on ionic strength within the interval 3 – 700 mM. Optimal performance was found at the lowest ionic strength evaluated. The response time was less than 4 minutes and the sensor was able to reversibly sense ammonium from μM to mM concentrations. The detection limit was $\sim 1 \times 10^{-6}$ M, i.e. about the same or even better than that reported for the best performing ion-selective electrodes. The preliminary estimate of precision at 200×10^{-6} M, using relative standard deviation (RSD) as a measure, was about 5 % over a ten-day period. The within-batch repeatability was about 2 % (RSD) at 200×10^{-6} M, comparable with the RSD between pixels. The image resolution was 210×10^{-6} m. In contrast to ISE's, the imaging sensor was able to cover a comparably large region of interest (3×10^{-4} m^2) with good spatial resolution (2.1×10^{-4} m). In addition, the

sensor was found selective for ammonium compared to the well known interfering ion i.e. potassium (mixed solution method; fixed primary ion: NH_4^+:K^+ ~ 17:1).

The normalization procedure (two-phase dual-excitation/dual-emission fluorescence reference scheme) was found to cancel out variations in fluorescence signal associated with excitation light intensity and pH, i.e. conditions frequently reported to alter performance of fluorescence based optical sensors. However, it was not possible to eliminate artifacts associated with fluctuations in temperature, effective MC 540 concentrations and sample ionic strength by the ratiometric reference scheme. MC540 is subject to the formation of non-fluorescent dimers and monomer - dimer complexation, which distort the fluorescence ratio.

Over an experimental period of ~ 10 days, the fluorescence intensity for each wavelength was reduced to ~ 15% of the initial fluorescence (t = 0). Based on the same data set, the corresponding fluorescence ratio decreased to ~ 75 % of the ratio measured at the start of experiments. Thus, the ratiometric procedure (without time correlation) compensated for most, but not all, of the signal drift observed for the individual wavelengths. The drift over time was on the other hand more or less completely removed using the time correlated pixel-by-pixel calibration protocol.

The time correlated pixel-by-pixel calibration (TCPC) technique was used to predict analytical sensitivity, limit of detection and determination of signal variation (relative standard deviation) at a pixel level throughout measurements without separate tests. The predicted parameters using TCPC agreed well with the determinations of the parameters using standard analytical protocols. In addition, detection limit from the TCPC protocol was used to define the operational lifetime of the sensor. However when exposed to a soil matrix the operational lifetime was reduced by 50 % to about 5 days. The decrease in sensor performance was efficiently tracked by all the statistical parameters during the experimental period. In addition, the images displaying the statistical parameters detection limit and analytical sensitivity could be used in conjunction with images of the relative signal variation of measured concentrations for image quality control at a high spatial and temporal resolution throughout measurements

The imaging optode was used to study ammonium turnover close to a root system of a tomato plant. In contrast to most other existing techniques, this method comprises a complete characterization of the ammonium turnover close to roots with a minimal and non-destructive manipulation of the root system. In addition, the same structure could be studied for relatively long periods including during plant growth.
Images of ammonium concentrations throughout the experiment made it possible to *i)* determine ammonium turnover rate of the root system; *ii)* visualize the ammonium depletion zone; *iii)* define the active ammonium uptake potential and; *iv)* localize active/inactive root structures. In addition to the fast characterization of ammonium turnover close to roots, the results indicated that most of the root system was active at the same time. Uptake proceeded over the entire root structure but the thin peripheral roots were about twice as efficient as the main root and were supported by a higher

supply. Overlapping root zones and framing of the supply by roots most likely influenced the positions of the depletion zones. Thus, the root arrangement greatly influenced the ammonium turnover close to this root system. The high relative standard error retrieved from the TCPC protocol indicated rapid concentration fluctuations in a peripheral part of a root structure.

The phase ratiometric optode design is benefited by the years of development of ion selective electrodes. Numerous ionophores already tested in electrodes could theoretically be used for imaging by a simple incorporation in the sensing film without altering the instrumental setup (Table 1). Fiber optic optodes based on the identical or a similar sensor configurations have previously been made for determination of potassium[69] (the original sensor design), nitrite[88] and chloride[71]. The technique facilitates high through put screening by simultaneous detection of optode arrays representing different analytes by using a single type of fluorescent dye as a signal transducer. In addition, coextraction based optodes using potential or solvent sensitive dyes could utilize a ratiometric sensing scheme and with time correlated pixel-by-pixel calibration be used for extended time for imaging with accompanying statistical measures of the signal quality. Thus, based on this versatile sensing scheme and calibration technique, many other important solutes found in complex environments could most likely be accurately detected with a comparably high coverage, spatial and temporal resolution.

Table 1. Examples of available ionophores for various solutes.

Available ionophores		
Cations	Anions	Molecules
H^+, NH_4^+, Cd^{2+}, Ca^{2+}, Li^+, Mg^{2+}, K^+, Na^+, Ba^{2+}, Cu^{2+},Pb^{2+}, Ag^+, Cs^+ , Br^-/Ca^{2+}	NO_2^-,Cl^-, CO_3^{2-}, Br^-	Amines, Uranyl

Acknowledgements

First of all I wish to thank Stefan Hulth for enthusiastic, ambitious and extraordinary supervision. It has been great fun to work with you during all these years. However, the outcome of this study would not have been conceivable without the discussion and criticism provided by a whole bunch of people at AMK. I especially want to thank Karen Andersson, Gustav Hulthe and Anders Loren for fruitful discussions and for their enthusiasm. I also acknowledge skilful assistance of Mattias and Roger Karlsson during the initial development of the ammonium sensor. I am also thankful to Frank Gilbert for letting me use the excellent CCD camera that was used for the imaging experiments.

Tobias Larsson is also one of the persons I have to acknowledge since I basically forced him to listen to endless monologues about strange response curves for about four years! I do not understand how you put up with all. Thanks for introducing me to Matlab.

Johan Engelbrektson, thanks for all help I have received during my Ph.D-studies ranging from broken coffee machines to LC-MS instruments.

Pia Engström, it has been a pleasure to work with you.

Aron, for reading manuscripts.

Mum and dad, for all support during almost 32 years and for the plants used in the experiments in this study.

Finally and most of all I have to give credit to Christina and Simon for their support, especially the last two months.

This study was financially supported by Swedish Natural Science Research Council (VR), the Foundation for Strategic Environmental Research (MISTRA), Swedish Research Council for Environment, Agricultural Sciences and Spatial Planning (FORMAS), the Swedish Engineering Foundation and the Technology Link Foundation (TBSG).

References

1. Salsac, L., Chaillou, S., Morotgaudry, J. F. & Lesaint, C. Nitrate and Ammonium Nutrition in Plants. *Plant Physiology and Biochemistry* **25**, 805-812 (1987).
2. Gazzarrini, S. et al. Three functional transporters for constitutive, diurnally regulated, and starvation-induced uptake of ammonium into arabidopsis roots. *Plant Cell* **11**, 937-947 (1999).
3. Aertebjerg, G. et al. in *Topic report European Environment Agency* (2001).
4. Sharpley, A. N., Sims, D. T., Lemunyon, J., Stevens, R. & Parry, R. in *Agricultural Research Service United State Department of Agriculture* (2003).
5. Herschel, S. J. F. W. On a case of superficial colour presented by a homogeneous liquid internally colourless. *Phil.Trans.R.Soc. London* **135**, 143-145 (1845).
6. Stokes, G. G. On the change of refrangibility of light. *Phil.Trans.R.Soc. London* **142**, 463-562 (1852).
7. Lakowicz, J. R. pp. 531-572 (Kluwer Academic / Plenum Publishers, New York, 1999).
8. Hunter, R. J. *Introduction to Modern Colloid Science* (Oxford University Press, Oxford, UK, 1999).
9. Shaw, D. J. *Introduction to colloid and surface chemistry* (Butterworths, London, 1980).
10. Eliasson, C. et al. Multivariate evaluation of doxorubicin surface-enhanced Raman spectra. *Spectrochimica Acta Part a-Molecular and Biomolecular Spectroscopy* **57**, 1907-1915 (2001).
11. Loren, A. et al. Feasibility of quantitative determination of doxorubicin with surface-enhanced Raman spectroscopy. *Journal of Raman Spectroscopy* **32**, 971-974 (2001).
12. Loren, A. et al. Internal standard in surface-enhanced Raman spectroscopy. *Analytical Chemistry* **76**, 7391-7395 (2004).
13. Lubbers, D. W. & Opitz, N. Po2-Optode, a New Tool to Measure Po2 of Biological Gases and Fluids by Quantitative Fluorescence Photometry. *Pflugers Archiv-European Journal of Physiology* **359**, R145-R145 (1975).
14. Lubbers, D. W. & Opitz, N. Ge))Pco2-Optode-Po2-Optode - New Probe for Measurement of Pco2 or Po2 in Fluids and Gases. *Zeitschrift Fur Naturforschung C-a Journal of Biosciences* **30**, 532-533 (1975).
15. Opitz, N. & Lubbers, D. W. New Fast-Responding Optical Method to Measure Pco2 in Gases and Solutions. *Pflugers Archiv-European Journal of Physiology* **355**, R120-R120 (1975).
16. Bergman, I. Rapid-Response Atmospheric Oxygen Monitor Based on Fluorescence Quenching. *Nature* **218**, 396-& (1968).
17. Hecht, E. *Optics* (Addison-Wesley, Reading, Mass., 1998).
18. Tan, W. H., Shi, Z. Y., Smith, S., Birnbaum, D. & Kopelman, R. Submicrometer Intracellular Chemical Optical Fiber Sensors. *Science* **258**, 778-781 (1992).
19. Kopelman, R., Tan, W. H. & Birnbaum, D. Subwavelength Spectroscopy, Exciton Supertips and Mesoscopic Light-Matter Interactions. *Journal of Luminescence* **58**, 380-387 (1994).
20. Clark, H. A., Hoyer, M., Philbert, M. A. & Kopelman, R. Optical nanosensors for chemical analysis inside single living cells. 1. Fabrication,

characterization, and methods for intracellular delivery of PEBBLE sensors. *Analytical Chemistry* **71**, 4831-4836 (1999).
21. Clark, H. A., Kopelman, R., Tjalkens, R. & Philbert, M. A. Optical nanosensors for chemical analysis inside single living cells. 2. Sensors for pH and calcium and the intracellular application of PEBBLE sensors. *Analytical Chemistry* **71**, 4837-4843 (1999).
22. Ng, R. H., Sparks, K. M. & Statland, B. E. Colorimetric Determination of Potassium in Plasma and Serum by Reflectance Photometry with a Dry-Chemistry Reagent. *Clinical Chemistry* **38**, 1371-1372 (1992).
23. Kim, S. B., Cho, H. C., Cha, G. S. & Nam, H. Microtiter plate-format optode. *Analytical Chemistry* **70**, 4860-4863 (1998).
24. Glud, R. N., Ramsing, N. B., Gundersen, J. K. & Klimant, I. Planar optrodes: A new tool for fine scale measurements of two- dimensional O_2 distribution in benthic communities. *Marine Ecology-Progress Series* **140**, 217-226 (1996).
25. Skoog, D. A., Holler, F. J. & Nieman, T. A. in *Principles of Instrumental Analysis* (ed. Messina, F.) pp. 99-114 (Saunders Collage Publishing, Philadelphia, 1998).
26. Peterson, J. I., Goldstein, S. R., Fitzgerald, R. V. & Buckhold, D. K. Fiber Optic Ph Probe for Physiological Use. *Analytical Chemistry* **52**, 864-869 (1980).
27. Guthrie, A. J., Narayanaswamy, R. & Russell, D. A. Application of Kubelka - Munk Diffuse Reflectance Theory to Optical Fiber Sensors. *Analyst* **113**, 457-461 (1988).
28. Wolfbeis, O. S. *Fiber optic chemical sensors and biosensors* (CRC Press, Boca Raton, Florida, USA, 1991).
29. Kirkbright, G. F., Narayanaswamy, R. & Welti, N. A. Fibre-Optic Ph Probe Based on the Use of an Immobilized Colorimetric Indicator. *Analyst* **109**, 1025-1028 (1984).
30. Sotomayor, M. D. T., DePaoli, M. A. & deOliveira, W. A. Fiber-optic pH sensor based on poly(o-methoxyaniline). *Analytica Chimica Acta* **353**, 275-280 (1997).
31. Miro, M., Frenzel, W., Estela, J. M. & Cerda, V. A novel flow-through disk-based solid-phase extraction diffuse reflectance optrode. Application to preconcentration and determination of trace levels of nitrite. *Analyst* **126**, 1740-1746 (2001).
32. Knoll, W. Interfaces and thin films as seen by bound electromagnetic waves. *Annual Review of Physical Chemistry* **49**, 569-638 (1998).
33. Maccraith, B. D. et al. Sol-Gel Coatings for Optical Chemical Sensors and Biosensors. *Sensors and Actuators B-Chemical* **29**, 51-57 (1995).
34. Holst, G. & Grunwald, B. Luminescence lifetime imaging with transparent oxygen optodes. *Sensors and Actuators B-Chemical* **74**, 78-90 (2001).
35. Burstein, E., Chen, W. P., Chen, Y. J. & Hartstein, A. Surface Polaritons - Propagating Electromagnetic Modes at Interfaces. *Journal of Vacuum Science & Technology* **11**, 1004-1019 (1974).
36. Kurihara, K., Nakamura, K., Hirayama, E. & Suzuki, K. An absorption-based surface plasmon resonance sensor applied to sodium ion sensing based on an ion-selective optode membrane. *Analytical Chemistry* **74**, 6323-6333 (2002).
37. Jordan, C. E., Frey, B. L., Kornguth, S. & Corn, R. M. Characterization of Poly-L-Lysine Adsorption onto Alkanethiol-Modified Gold Surfaces with

Polarization-Modulation Fourier-Transform Infrared-Spectroscopy and Surface-Plasmon Resonance Measurements. *Langmuir* **10**, 3642-3648 (1994).
38. Ligler, F. S. & Taitt, C. A. R. *Optical biosensors : present and future* (Elsevier, Amsterdam ; New York, 2002).
39. Rothenhausler, B. & Knoll, W. Surface-Plasmon Microscopy. *Nature* **332**, 615-617 (1988).
40. Jordan, C. E. & Corn, R. M. Surface plasmon resonance imaging measurements of electrostatic biopolymer adsorption onto chemically modified gold surfaces. *Analytical Chemistry* **69**, 1449-1456 (1997).
41. Kurihara, K. & Suzuki, K. Theoretical understanding of an absorption-based surface plasmon resonance sensor based on Kretchmann's theory. *Analytical Chemistry* **74**, 696-701 (2002).
42. Vukusic, P. S. & Sambles, J. R. Cobalt Phthalocyanine as a Basis for the Optical Sensing of Nitrogen-Dioxide Using Surface-Plasmon Resonance. *Thin Solid Films* **221**, 311-317 (1992).
43. Chadwick, B., Tann, J., Brungs, M. & Gal, M. A Hydrogen Sensor-Based on the Optical-Generation of Surface-Plasmons in a Palladium Alloy. *Sensors and Actuators B-Chemical* **17**, 215-220 (1994).
44. Homola, J., Yee, S. S. & Gauglitz, G. Surface plasmon resonance sensors: review. *Sensors and Actuators B-Chemical* **54**, 3-15 (1999).
45. Brockman, J. M., Nelson, B. P. & Corn, R. M. Surface plasmon resonance imaging measurements of ultrathin organic films. *Annual Review of Physical Chemistry* **51**, 41-63 (2000).
46. Kautsky, H. & Hirsch, A. Nachweis geringster Sauer-stoffmengen durch Phophoreszenztilgung. *Z. fur anorg allgem Chemie* **222**, 126-134 (1935).
47. Hargittai, P. T., Ginty, D. D. & Lieberman, E. M. A Pyrene Fluorescence Technique and Microchamber for Measurement of Oxygen-Consumption of Single Isolated Axons. *Analytical Biochemistry* **163**, 418-426 (1987).
48. Opitz, N. & Lubbers, D. W. Increased Resolution Power in Po2 Analysis at Lower Po2 Levels Via Sensitivity Enhanced Optical Po2 Sensors (Po2 Optodes) Using Fluorescence Dyes. *Advances in Experimental Medicine and Biology* **180**, 261-267 (1984).
49. Opitz, N. & Lubbers, D. W. Evidence for Boundary-Layer Effects Influencing the Sensitivity of Microencapsulated O-2 Fluorescence Indicator Molecules. *Advances in Experimental Medicine and Biology* **169**, 899-905 (1984).
50. Wolfbeis, O. S. & Carlini, F. M. Long-Wavelength Fluorescent Indicators for the Determination of Oxygen Partial Pressures. *Analytica Chimica Acta* **160**, 301-304 (1984).
51. Podgorski, G. T., Longmuir, I. S., Knopp, J. A. & Benson, D. M. Use of an Encapsulated Fluorescent-Probe to Measure Intracellular Po2. *Journal of Cellular Physiology* **107**, 329-334 (1981).
52. Bacon, J. R. & Demas, J. N. Determination of Oxygen Concentrations by Luminescence Quenching of a Polymer-Immobilized Transition-Metal Complex. *Analytical Chemistry* **59**, 2780-2785 (1987).
53. Klimant, I. & Wolfbeis, O. S. Oxygen-Sensitive Luminescent Materials Based on Silicone-Soluble Ruthenium Diimine Complexes. *Analytical Chemistry* **67**, 3160-3166 (1995).
54. Lippitsch, M. E., Pusterhofer, J., Leiner, M. J. P. & Wolfbeis, O. S. Fibre-Optic Oxygen Sensor with the Fluorescence Decay Time as the Information Carrier. *Analytica Chimica Acta* **205**, 1-6 (1988).

55. Klimant, I., Meyer, V. & Kuhl, M. Fiberoptic Oxygen Microsensors, a New Tool in Aquatic Biology. *Limnology and Oceanography* **40**, 1159-1165 (1995).
56. Douglas, P. & Eaton, K. Response characteristics of thin film oxygen sensors, Pt and Pd octaethylporphyrins in polymer films. *Sensors and Actuators B-Chemical* **82**, 200-208 (2002).
57. Pollok, B. A. & Heim, R. Using GFP in FRET-based applications. *Trends in Cell Biology* **9**, 57-60 (1999).
58. Peyker, A., Rocks, O. & Bastiaens, P. I. H. Imaging activation of two Ras isoforms simultaneously in a single cell. *Chembiochem* **6**, 78-85 (2005).
59. Lee, S. H. et al. Calix 4 crown in dual sensing functions with FRET. *Tetrahedron Letters* **46**, 8163-8167 (2005).
60. Ueyama, H., Takagi, M. & Takenaka, S. A novel potassium sensing in aqueous media with a synthetic oligonucleotide derivative. Fluorescence resonance energy transfer associated with guanine quartet-potassium ion complex formation. *Journal of the American Chemical Society* **124**, 14286-14287 (2002).
61. Bambot, S. B., Sipior, J., Lakowicz, J. R. & Rao, G. Lifetime-Based Optical Sensing of Ph Using Resonance Energy-Transfer in Sol-Gel Films. *Sensors and Actuators B-Chemical* **22**, 181-188 (1994).
62. Medintz, I. L. et al. Self-assembled nanoscale biosensors based on quantum dot FRET donors. *Nature Materials* **2**, 630-638 (2003).
63. Tsien, R. Y. & Poenie, M. Fluorescence Ratio Imaging - a New Window into Intracellular Ionic Signaling. *Trends in Biochemical Sciences* **11**, 450-455 (1986).
64. Grynkiewicz, G., Poenie, M. & Tsien, R. Y. A New Generation of Ca-2+ Indicators with Greatly Improved Fluorescence Properties. *Journal of Biological Chemistry* **260**, 3440-3450 (1985).
65. Hulth, S., Aller, R. C., Engstrom, P. & Selander, E. A pH plate fluorosensor (optode) for early diagenetic studies of marine sediments. *Limnology and Oceanography* **47**, 212-220 (2002).
66. Kikuchi, K., Takakusa, H. & Nagano, T. Recent advances in the design of small molecule-based FRET sensors for cell biology. *Trac-Trends in Analytical Chemistry* **23**, 407-415 (2004).
67. Zhu, Q. Z., Aller, R. C. & Fan, Y. Z. High-performance planar pH fluorosensor for two-dimensional pH measurements in marine sediment and water. *Environmental Science & Technology* **39**, 8906-8911 (2005).
68. Sumiyoshi, H. & Nakahara, K. New convinient colorometric determination of potassium in blood serum. *Talanta* **24**, 763-765 (1977).
69. Krause, C., Werner, T., Huber, C., Wolfbeis, O. S. & Leiner, M. J. P. pH-insensitive ion selective optode: A coextraction-based sensor for potassium ions. *Analytical Chemistry* **71**, 1544-1548 (1999).
70. Krause, C., Werner, T. & Wolfbeis, O. S. Multilayer potassium sensor based on solid-state coextraction. *Analytical Sciences* **14**, 163-167 (1998).
71. Huber, C., Werner, T., Krause, C., Wolfbeis, O. S. & Leiner, M. J. P. Overcoming the pH dependency of optical sensors: a pH- independent chloride sensor based on co-extraction. *Analytica Chimica Acta* **398**, 137-143 (1999).

72. He, H. R. et al. Novel Type of Ion-Selective Fluorosensor Based on the Inner Filter Effect - an Optrode for Potassium. *Analytical Chemistry* **65**, 123-127 (1993).
73. Montana, V., Farkas, D. L. & Loew, L. M. Dual-Wavelength Ratiometric Fluorescence Measurements of Membrane-Potential. *Biochemistry* **28**, 4536-4539 (1989).
74. Gross, E., Bedlack, R. S. & Loew, L. M. Dual-Wavelength Ratiometric Fluorescence Measurement of the Membrane Dipole Potential. *Biophysical Journal* **67**, 208-216 (1994).
75. Sikurova, L. & Frankova, R. Temperature Induced Changes in Monomer-Dimer Distribution of Merocyanine-540 in Dimyristoyl Lecithin Liposomes. *Studia Biophysica* **140**, 21-28 (1991).
76. Thompson, R. B., Maliwal, B. P., Feliccia, V. L., Fierke, C. A. & McCall, K. Determination of picomolar concentrations of metal lons using fluorescence anisotropy: Biosensing with a "reagentless" enzyme transducer. *Analytical Chemistry* **70**, 4717-4723 (1998).
77. Lakowicz, J. R., Gryczynski, I., Gryczynski, Z. & Dattelbaum, J. D. Anisotropy-based sensing with reference fluorophores. *Analytical Biochemistry* **267**, 397-405 (1999).
78. Harms, G. S., Sonnleitner, M., Schutz, G. J., Gruber, H. J. & Schmidt, T. Single-molecule anisotropy imaging. *Biophysical Journal* **77**, 2864-2870 (1999).
79. Zeng, H. H. et al. Real-time determination of picomolar free Cu(II) in seawater using a fluorescence based fiber optic biosensor. *Analytical Chemistry* **75**, 6807-6812 (2003).
80. Szmacinski, H. & Lakowicz, J. R. Fluorescence Lifetime-Based Sensing and Imaging. *Sensors and Actuators B-Chemical* **29**, 16-24 (1995).
81. Lampert, R. A. et al. Standards for Nanosecond Fluorescence Decay Time Measurements. *Analytical Chemistry* **55**, 68-73 (1983).
82. Holst, G. et al. A modular luminescence lifetime imaging system for mapping oxygen distribution in biological samples. *Sensors and Actuators B-Chemical* **51**, 163-170 (1998).
83. Tengberg, A. et al. Evaluation of a lifetime-based optode to measure oxygen in aquatic systems. *Limnology and Oceanography-Methods* **4**, 7-17 (2006).
84. Liebsch, G., Klimant, I., Krause, C. & Wolfbeis, O. S. Fluorescent imaging of pH with optical sensors using time domain dual lifetime referencing. *Analytical Chemistry* **73**, 4354-4363 (2001).
85. Mayr, T., Klimant, I., Wolfbeis, O. S. & Werner, T. Dual lifetime referenced optical sensor membrane for the determination of copper(II) ions. *Analytica Chimica Acta* **462**, 1-10 (2002).
86. Huber, C. et al. Optical sensor for seawater salinity. *Fresenius Journal of Analytical Chemistry* **368**, 196-202 (2000).
87. Huber, C., Klimant, I., Krause, C. & Wolfbeis, O. S. Dual lifetime referencing as applied to a chloride optical sensor. *Analytical Chemistry* **73**, 2097-2103 (2001).
88. Huber, C., Klimant, I., Krause, C., Werner, T. & Wolfbeis, O. S. Nitrate-selective optical sensor applying a lipophilic fluorescent potential-sensitive dye. *Analytica Chimica Acta* **449**, 81-93 (2001).

89. Scheenen, W., Makings, L. R., Gross, L. R., Pozzan, T. & Tsien, R. Y. Photodegradation of indo-1 and its effect on apparent Ca^{2+} concentrations. *Chemistry & Biology* **3**, 765-774 (1996).